Botanical Journal of the Linnean Society, 2004, **145**, 295–316. With 80 figures

Comparative anatomy and morphology of fertile complexes of *Prumnopitys* and *Afrocarpus* species (Podocarpaceae) as revealed by histology and NMR imaging, and their relevance to systematics

ROBERT R. MILL FLS[1]*, MICHAEL MÖLLER[1], SHEILA M. GLIDEWELL[2], DIANE MASSON[2] and BRIAN WILLIAMSON[2]

[1]*Royal Botanic Garden Edinburgh, 20A Inverleith Row, Edinburgh EH3 5LR, UK*
[2]*Scottish Crop Research Institute, Invergowrie, Dundee DD2 5DA, UK*

Received July 2003; accepted for publication January 2004

Fertile complexes (individual reproductive units of ovulate cones) of three *Prumnopitys* species and *Afrocarpus falcatus* (Podocarpaceae) were subjected to histological examination and non-destructive NMR imaging. The latter technique allowed the display, frame-by-frame analysis and electronic 'dissection' of internal structures such as the number and courses of vascular traces and resin canals and their morphology. Characters of these internal structures distinguished all three *Prumnopitys* species from each other and thus were shown to be taxonomically diagnostic. Fertile complexes of *Prumnopitys andina* and *P. taxifolia* were most similar, possessing simple vascular traces and few unbranched resin canals. Those of *P. ferruginea* were very different and possessed an interconnected network of resin ducts within the sarcotesta. These findings are congruent with relationships inferred from molecular phylogenetic studies, in which two subclades were recovered within *Prumnopitys*. The anatomy of the female fertile complexes of *Afrocarpus falcatus* was very distinct from all *Prumnopitys* species analysed. Its most distinctive feature was the existence of a complex network of radial vascular strands originating from within the outer layers of the sarcotesta and penetrating the inner layers of the fertile complex. The surface texture and morphology of the sclerotesta of the seed was also unique to each species. *Botanical Journal of the Linnean Society*, 2004, **145**, 295–316.

ADDITIONAL KEYWORDS: epimatium – idioblasts – New Zealand – resin canals – sarcotesta – sclerotesta – South Africa – South America – *Sundacarpus* – vasculature.

INTRODUCTION

All genera of the Podocarpaceae (commonly referred to as 'podocarps') differ from most other conifers (e.g. Pinaceae and Araucariaceae) in having non-woody, more or less fleshy, female fertile bract–scale complexes (Tomlinson & Takaso, 2003). In some taxa these are borne in multi-ovulate cones that are either loose and spike-like (e.g. some species of *Prumnopitys* such as *P. taxifolia* (Banks & Sol. ex D. Don) de Laub.: Morvan, 1983) or compact (e.g. *Microcachrys*: Morvan, 1990), but in the majority they are borne singly, as in *Afrocarpus* and most species of *Podocarpus*.

In this study we compare the anatomy of the fertile complexes of three species of *Prumnopitys* [*P. andina* (Poepp. ex Endl.) de Laub., *P. taxifolia* and *P. ferruginea* (G. Benn. ex D. Don) de Laub.] and one of *Afrocarpus* [*A. falcatus* (Thunb.) C.N. Page]. *P. ferruginea* and all species of *Afrocarpus* have single-ovulate cones and the terms 'ovule' and 'cone' are thus synonymous (though not homologous), whereas *P. andina* and *P. taxifolia* have multi-ovulate cones in which the female fertile shoot bears several ovules in a spicate 'infructescence', which *in toto* has been called the cone by most previous workers (e.g. Morvan, 1983; Tomlinson, 1992). In all four species studied, we examined single reproductive units. Hence we have here followed Tomlinson (1992) and Tomlinson & Takaso (2003) in using the expression 'fertile complex' to

*Corresponding author. E-mail: R.Mill@rbge.org.uk

denote the structures that we studied, which were called 'cones' in Glidewell *et al*. (2002); we here restrict 'cone' to the entire reproductive structure.

In most Podocarpaceae, the ovule is supported on a structure called the epimatium, which is considered homologous with the ovuliferous scale of other conifers such as *Pinus* and in many genera also serves to invert the ovule in early developmental stages (Tomlinson, 1992). Together with the integumentary tissue, the epimatium is vascularized (Tomlinson & Takaso, 2003) but, as in other living conifers, the nucellus and megagametophyte are not. In both *Prumnopitys* and *Afrocarpus*, the epimatium is more or less completely fused to the integumentary tissue. The outer integumentary layers (and fused epimatium) of these fertile complexes are more or less fleshy in later stages of development and then collectively act as a sarcotesta that, when ripe, is brightly coloured to attract animal dispersal vectors.

Between the sarcotesta and megagametophyte, a very hard middle layer (sclerotesta) develops during the resting phase of fertile complex development in both genera, as described for *Acmopyle* by Mill *et al*. (2001). This hard layer greatly hampers anatomical examination of female podocarp fertile complexes at this or later stages, when conventional sectioning of whole fertile complexes becomes impossible, though very young ovules with immature sclerotesta can be sectioned. However, data obtained from such young stages should not be used to infer the anatomy of the fully developed fertile complex.

The fleshiness and liquid content of podocarp fertile complexes make them suitable subjects for nuclear magnetic resonance (NMR) imaging techniques. Previously, NMR imaging has chiefly been used in studies of commercially important plants whose taxonomy is uncontroversial (for examples see the overview by Ishida, Koizumi & Kano, 2000). These methods are non-destructive and non-invasive, yet reveal three-dimensional images of the vascular supply and resin or mucilage canals within the fertile complexes as well as their internal layering. Several recent papers have demonstrated the potential capabilities of NMR imaging techniques as tools to investigate aspects of the biology of the Podocarpaceae, including pollination mechanisms (Möller *et al*., 2000), development of fertile complexes (Mill *et al*., 2001) and examination of herbarium material (Masson *et al*., 2001). To investigate the potential of NMR imaging combined with conventional anatomical techniques to solve taxonomic problems in this family, we have conducted a case study on three species currently classified in *Prumnopitys*, with *Afrocarpus* used for comparison. The NMR techniques and parameters used in this study were discussed in detail elsewhere (Glidewell *et al*., 2002). The work reported here is an extension of that study and focuses more on the morphological and anatomical differences observed between the species. The aims of the study were to test the validity of previously recognized subgroups within *Prumnopitys* and to test intergeneric relationships inferred from recent molecular phylogenetic studies (Sinclair *et al*., 2002).

The nine extant species of *Prumnopitys* (Farjon, 2001) are disjunctly distributed between South and Central America (five species) and Australasia (four). *P. andina* (one of whose synonyms, *P. elegans* Phil., is the type of the genus) grows in Chile and Argentina; *P. montana* (Humb. & Bonpl. ex Willd.) de Laub. and three others occur in west-tropical South America and Central America. The Australasian species comprise two in New Zealand (*P. taxifolia* and *P. ferruginea*), and one each in Australia [*P. ladei* (F.M. Bailey) de Laub.] and New Caledonia [*P. ferruginoides* (Compton) de Laub.]. *Afrocarpus* comprises several ill-defined species: *A. falcatus* (the type) in southern Africa, *A. gracilior* (Pilg.) C.N. Page and two others in eastern tropical and Highlands Africa, *A. mannii* (Hook. f.) C.N. Page on São Tomé and *A. gaussenii* (Woltz) C.N. Page on Madagascar.

For many years, *Prumnopitys* and *Afrocarpus* were both treated as sections of a very broadly delimited genus *Podocarpus*, respectively, as *P.* sect. *Stachycarpus* (Buchholz & Gray, 1948a, b; Gray & Buchholz, 1951a) and *P.* sect. *Afrocarpus* (Buchholz & Gray, 1948a; Gray, 1953). *Prumnopitys* first received an approximation to its present delimitation by de Laubenfels (1978); besides the species now generally accepted as belonging to it, he also included an additional species, *P. amara* (Blume) de Laub., which is separated generically as *Sundacarpus amarus* (J. Buchholz & N.E. Gray) C.N. Page by many recent authorities (e.g. Page, 1989, 1990; Bobrov & Romanov, 1999; Melikian & Bobrov, 2000; Farjon, 2001) although this segregation has not been universally accepted (e.g. de Laubenfels, 1978; Kelch, 2002). The most recent proposal, by Melikian & Bobrov (2000), divided *Prumnopitys* in the sense of Page (1990) into three genera. Three South American species, plus *P. taxifolia*, were placed by Melikian and Bobrov in *Prumnopitys s.s.*; the Australasian species (except *P. taxifolia*) became *Stachypitys*; and the *P. montana* species complex of South America was named *Van-Tieghemia* (itself renamed *Botryopitys* by Doweld, 2001, because *Van-Tieghemia* was illegitimate). *Afrocarpus* is now also usually regarded as a distinct genus (e.g. Page, 1990; Hill & Pole, 1992; Tomlinson, 1992, 1994; Farjon, 2001).

Since both *Prumnopitys* and *Afrocarpus* have become accepted as genera, neither has been regarded as closely allied to the other, except that Bobrov & Romanov (1999) and Melikian & Bobrov (2000) noted similarities between the fertile complexes of *Afrocar-*

pus and *Sundacarpus*, but not between *Afrocarpus* and *Prumnopitys*. Molecular phylogenetic studies (Kelch, 1998, 2002; Conran *et al*., 2000; Sinclair *et al*., 2002) also place *Afrocarpus* and the *Prumnopitys–Sundacarpus* group in separate clades within the family. For this reason, and because fresh material was available, *Afrocarpus* was chosen as a reference with which to compare the various species of *Prumnopitys*.

MATERIAL AND METHODS

Plant material

Living cone-bearing material of three species of *Prumnopitys* was studied. Material of *P. ferruginea* and *P. taxifolia* was sent by air from New Zealand in batches from January to March 1999. The material of *P. andina* came from an old tree in the Royal Botanic Garden Edinburgh (RBGE: accession number 19698199), which for many years has produced abundant male cones but in August 1999 was fortuitously discovered to be bearing several female cones comprising in all about 12 ovules, on three separate branches. For comparison, *Afrocarpus falcatus* was chosen, because its fertile complexes were outwardly similar in shape and size to those of *P. andina* and *P. taxifolia*; cones of *A. falcatus* were collected from a plantation on St Helena in June 1999. The material of *P. ferruginea* and *A. falcatus* was also used in the study reported by Glidewell *et al*. (2002). Fresh material of *Sundacarpus* and the tropical American group of *Prumnopitys* was not available.

NMR methods

Fertile complexes were imaged in 15- or 20-mm-diameter coils at 7.1 T in the microimaging probe of a Bruker AMX300 SWB NMR spectrometer (Bruker U.K. Ltd). No sample preparation was required and samples were held in place by tissue or foam. Single slice images and 128^3 3D datasets with a range of relaxation weightings were acquired for each specimen. Full details of the technique are given in Glidewell *et al*. (1997, 2002).

Histological methods and terminology

NMR images were validated using conventional freeze-sectioning histological methods, as described by Glidewell *et al*. (2002). In all species examined, microtome sectioning was limited largely to the sarcotesta and epidermis because of the hardness of the sclerotesta in fertile complexes that had reached the age of those used in the study, and so data are mainly limited to those regions. Fertile complexes could be cut open with some difficulty using a Proxxon Minimod 40E miniature circular saw as described for *Acmopyle pancheri* (Brongn. & Gris) Pilg. by Mill *et al*. (2001), but this method did not allow complete thin or serial sections of them to be obtained.

Histological sections were prepared in two ways. Some were cleared in bleach and then stained with safranin/fast green for standard histological examination. To test for starch grains, other sections (from the same samples) were mounted, without prior clearing, in Melzer's Reagent (1.5 g iodine, 5 g potassium iodide, 100 g chloral hydrate, 100 mL water) and observed under a Zeiss Axiophot microscope by bright-field and differential interference contrast (DIC) microscopy.

Histological terminology follows Mill *et al*. (2001). The outer layers (including the epidermis and hypodermis) functionally constitute the sarcotesta (= 'outer sarcotesta' of Sporne, 1974). Because in this paper we discuss only the outer sarcotesta in Sporne's sense, we refer to this simply as the sarcotesta. We have, however, used the expressions 'inner' and 'outer' as qualifiers, to refer to zones or layers within the sarcotesta (between, but not including, the hypodermis and the sclerotesta). Our usage is therefore similar to that of Andrews & Felix (1952) and the expression 'inner sarcotesta' as used here never refers to the endotesta, which has sometimes been termed the inner sarcotesta (e.g. by Sporne, 1974). Throughout this paper, we have used 'layer' to denote tissue regions delimited by histology, and 'zone' to denote regions delimited by NMR imaging.

The seeds of *Prumnopitys* are platyspermic (i.e. bilaterally symmetrical), with two longitudinal planes. The first of these (principal plane of Arber, 1910; major plane of Grove & Rothwell, 1980, and other recent authors) traverses the longer axis of the transverse section, and the second (secondary plane of Arber, 1910; minor plane of Grove & Rothwell, 1980, and others) traverses its shorter axis. Because most recent papers have used the terms major and minor planes, that terminology has been used here; it is widely used in palaeobotanical literature but most work dealing with extant Podocarpaceae has ignored the two planes of their seeds. The seeds of *Afrocarpus* are also platyspermic but are very much more symmetrical and could easily be misinterpreted as radiospermic (i.e. radially symmetrical), particularly if the whole fertile complex rather than the seed within is examined. The informal term kernel is used to denote collectively all tissues contained within the sarcotesta (i.e. the sclerotesta, endotesta, nucellus, megagametophyte and embryo).

Photography and imaging

Images were captured both on film and digitally. For film images obtained by microscopy, Fujichrome 64T

ISO 64 tungsten balanced slide film was used in a camera attachment fitted to either a Zeiss Stemi 2000C stereomicroscope or a Zeiss Axiophot compound microscope. Digital images were captured using a Kodak MegaPlus ES1.0 digital camera (resolution: 1008×1018 pixels) attached to a Zeiss Axiophot microscope.

RESULTS

The observed differences in histology and vasculature between all four studied species are summarized in Table 1. Data from NMR imaging and histology have been combined to build up as total a description as possible of the internal structures observed. A more detailed illustration of the NMR results, including animations, can be accessed at www.blackwellpublishing.com/products/journals/suppmat/BOJ/BOJ289/BOJ289sm.htm.

PRUMNOPITYS ANDINA

The fertile complex of *P. andina* examined was 11 mm in diameter and ovoid-spherical. At its topographical apex (morphologically, the basal or chalazal end, because of ovule inversion) was a small but pronounced knob (Fig. 1).

The kernel was 8 mm long, 8 mm wide in the major plane and 6.5 mm thick in the minor plane (Figs 8–11), with a relatively smooth, homogeneous brown surface (Fig. 12). At the micropylar end, a softer, darker area was present (Fig. 10, right), which could be easily removed, revealing a simple system of straight chambers (Fig. 10, left). Along its sides the kernel had two grooves (Figs 8–11), where the descending vascular bundles were situated (Fig. 29).

The internal structure of the fertile complexes appeared relatively simple in NMR images. In T_2-weighted images, the outer part of the embryo appeared bright in the centre of the megagametophyte, which was surrounded by a bright endotesta (Figs 28–30). In T_1-weighted images, the relative intensities of the outer embryo and megagametophyte were reversed (Fig. 30, right). Encircling the endotesta was a dark ring, the sclerotesta, which consisted of dense sclerified cells (Fig. 44). The sarcotesta could be differentiated into four zones by T_2-weighted NMR imaging (Figs 28, 29, 73). Around the periphery of the fertile complex was a narrow zone, slightly brighter than the other three (Figs 28, 29). Next were a wide, variegated outer zone and an inner zone of fairly uniform intensity; these were separated from each other by a thinner, darker transition zone that was not sharply defined and frequently penetrated the outer zone (Fig. 29). The vascular traces were located on the inner periphery of this transition zone (Figs 28, 29). In T_1-weighted images, the peripheral zone was bright, the transition zone was less evident and the inner zones were more uniform and of low intensity in which the vascular bundles appeared bright in contrast (Fig. 30, right).

Histological sections revealed a more complex differentiation of tissues (Figs 44, 73). The peripheral zone revealed by NMR imaging (Fig. 73, NMR zone 1) comprised the cuticle, epidermis and 4–7 hypodermal layers consisting of densely packed thick-walled collenchymatous cells (Figs 46, 47). The epidermal cells had a thick cuticle with deep incursions between their anticlinal walls (Fig. 47). The outermost of the two outer sarcotesta zones (Figs 29, 73, NMR zone 2) consisted of larger, thin-walled, radially elongated, parenchymatous cells filled with starch grains (Fig. 45). The inner one (Fig. 73, NMR zone 4) consisted of two cell layers, an inner layer of densely packed, thin-walled cells that appeared square in transverse section and an outer one of rounder thin-walled cells of similar size. The narrow transition zone between the two main zones (Figs 44, 73, NMR zone 3) was composed of thin-walled cells that were square in transverse section and stained dark blue–green with safranin/fast green. A few cells with possible tannin deposits were present in the sarcotesta, but only at the base of the fertile complex (Fig. 48). Towards the base of the fertile complex, an innermost sarcotestal layer of large, polygonal, radially elongated thin-walled cells was also present (Fig. 73, zone 5/layer 7); many of these cells had transverse striations, which could have been artefacts due to stress and tearing during sectioning.

In transverse NMR 'slices' in the equatorial plane of the fertile complex, the two ascending vascular traces just inside the transition zone were more distant from the sclerotesta than the two descending traces (Figs 29, 77). Near the chalazal apex, the ascending traces divided (Fig. 31) and a minor branch continued to ascend into the chalazal knob (Fig. 31, arrowed), whereas the main branch descended on the adaxial side. Maximum intensity projections and surface-rendered NMR images show the course of the traces in relation to the megagametophyte (Fig. 31, www.blackwellpublishing.com/products/journals/suppmat/BOJ/BOJ289/BOJ289sm.htm). The vascular bundles themselves were collateral (Fig. 50).

Resin canals were not obvious from either NMR or conventional histology. Only at the topographical base of the fertile complex were two residual ducts detected, each in association with a vascular trace (Fig. 49). These canals, however, did not reach the level of the sclerotesta (Fig. 50).

Starch grains in *P. andina* were irregular and nugget-shaped, *c.* 10 μm in length (Fig. 45), with pronounced lateral facets when seen using DIC (not shown).

Table 1. Comparison of the main characters differentiating four species of Podocarpaceae as revealed by NMR imaging and conventional sectioning

	Prumnopitys andina	*Prumnopitys taxifolia*	*Prumnopitys ferruginea*	*Afrocarpus falcatus*
Sarcotesta				
NMR zones	4 at equator, 5 near base	3	4 (the innermost as two crescents)	3
Histological layers	6 at equator, 7 near base	4	6 (the innermost as two crescents)	5
Sclerotesta (outside)	Smooth	Irregular outline	Smooth (with depressions corresponding to crescents)	Regularly convex protuberances
Hypodermal layers	4–7	3	1–3	1 or 2
'Resin' canal occurrence	Rudimentary at base in outer sarcotesta, layer 5 (1 per vascular trace)	In outer sarcotesta: 2 or 3 canals, 1 per vascular trace, plus 1 between traces only at the base	Interconnected network forming a ring in outer sarcotesta	(1) Two systems of branched pockets in outer sarcotesta layers 3 and 4 (2) In inner sarcotesta
Vascular traces	2 ascending and 2 descending (total 4)	2 ascending and 2 descending (total 4)	2 ascending and 2 descending (total 4)	4 ascending, at least 6 descending and bifurcating (total 10–14)
	Branched at chalazal end into knob	Branched at chalazal end into knob (Morvan, 1980, 1983)*	Branched at chalazal end with small bundle entering base of ovule (Sinnott, 1913: diagram 3F)*	Multiple branches laterally and inwards (radial strands) passing through the sclerotesta in close proximity to megagametophyte
Sclereids	None seen	None seen	None seen	Brachysclereids of *Juniperus* type
Starch grains	Present: in layers 3–5, in parenchyma	Limited to cells in a semicircle around the vascular traces (layer 3)	Present in layer 6 (vestigial inner sarcotesta layer) only	None observed in any histological layer
Epidermis cells	Elongated periclinally	Elongated periclinally	Irregularly isodiametric	Irregularly isodiametric
Chalazal knob	Present	Present	Present	Not evident

*Branching not observed in NMR images.

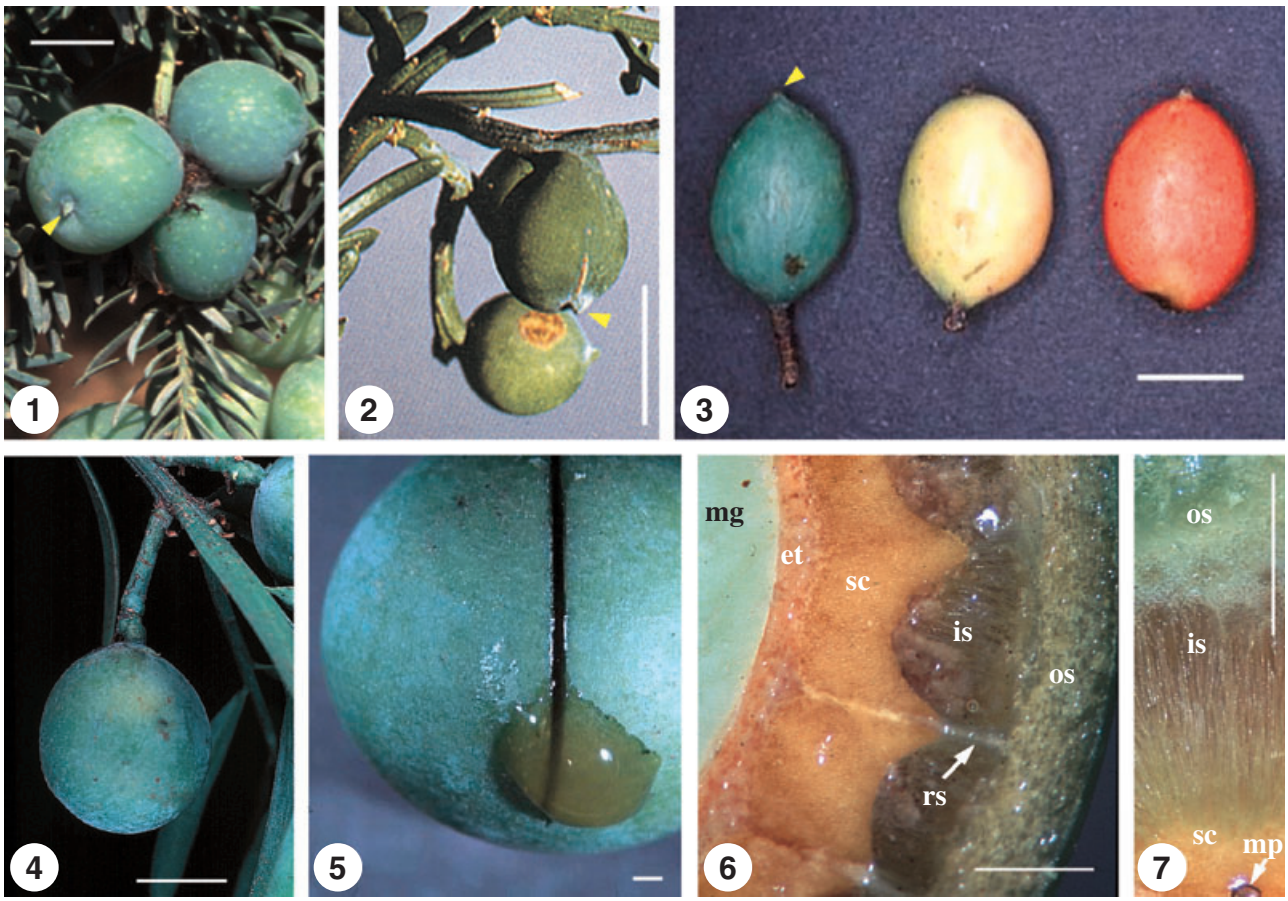

Figures 1–7. Morphology and anatomy of fertile complexes of *Prumnopitys* spp. and *Afrocarpus falcatus*. Fig. 1. *Prumnopitys andina*. External morphology, cone with three fertile complexes. Scale bar = 1 cm. Fig. 2. *Prumnopitys taxifolia*. External morphology, cone with two fertile complexes. Scale bar = 1 cm. Fig. 3. *Prumnopitys ferruginea*. Three fertile complexes at different stages of ripeness (left, unripe but close to maturity; middle, nearly ripe; right, ripe). Scale bar = 1 cm. Fig. 4. *Afrocarpus falcatus*. Cone showing peduncle bearing sterile bracts and single fertile complex. Scale bar = 1 cm. Fig. 5. *Afrocarpus falcatus*. Gum oozing from cut in sarcotesta of fertile complex. Scale bar = 100 µm. Fig. 6. *Afrocarpus falcatus*. Transverse section through fertile complex showing endotesta, sclerotesta and sarcotesta layers. Scale bar = 1 mm. Fig. 7. *Afrocarpus falcatus*. Close-up of inner sarcotesta layer showing gum deposits. Scale bar = 1 mm. Arrowheads in Figs 1–3 indicate chalazal knob. et – endotesta, is – inner sarcotesta layer, mg – megagametophyte, mp – micropyle, os – outer sarcotesta layer, rs – radial strand, sc – sclerotesta.

Prumnopitys taxifolia

Fertile complexes of *P. taxifolia* were more or less spherical, but with a pronounced knob at the topographical apex, or chalazal end (Fig. 2); the example measured was 8.5 mm in diameter.

The kernel of this species was the smallest of the four studied, at 7 mm long × 6 mm wide (major plane) × 5.5 mm thick (minor plane) (Figs 13–16). The most prominent feature was its irregular, light brown surface ornamentation, very unlike the much

Figures 8–27. Sclerotesta morphology of fertile complexes of *Prumnopitys* spp. and *Afrocarpus falcatus*. Figs 8–12. *Prumnopitys andina*; in Fig. 10 left split image – sclerotesta partially removed. Figs 13–17. *Prumnopitys taxifolia*. Figs 18–22. *Prumnopitys ferruginea*; in Figs 18, 20 left split image – inner, vestigial sarcotesta layer still attached to sclerotesta, right split image – inner, vestigial sarcotesta layer removed. Figs 23–27. *Afrocarpus falcatus*. Top row (Figs 8, 13, 18, 23), longitudinal views in major plane; second row (Figs 9, 14, 19, 24), longitudinal views in minor plane; middle row (Figs 10, 15, 20, 25), transverse views centred on micropyle; fourth row (Figs 11, 16, 21, 26), transverse views centred on chalaza; bottom row (Figs 12, 17, 22, 27), close-up of sclerotesta. Arrowheads (Fig. 8) – grooves. All scale bars = 1 mm; that in Fig. 8 also applies to Figs 9–11, 13–16, 18–21 and 23–26.

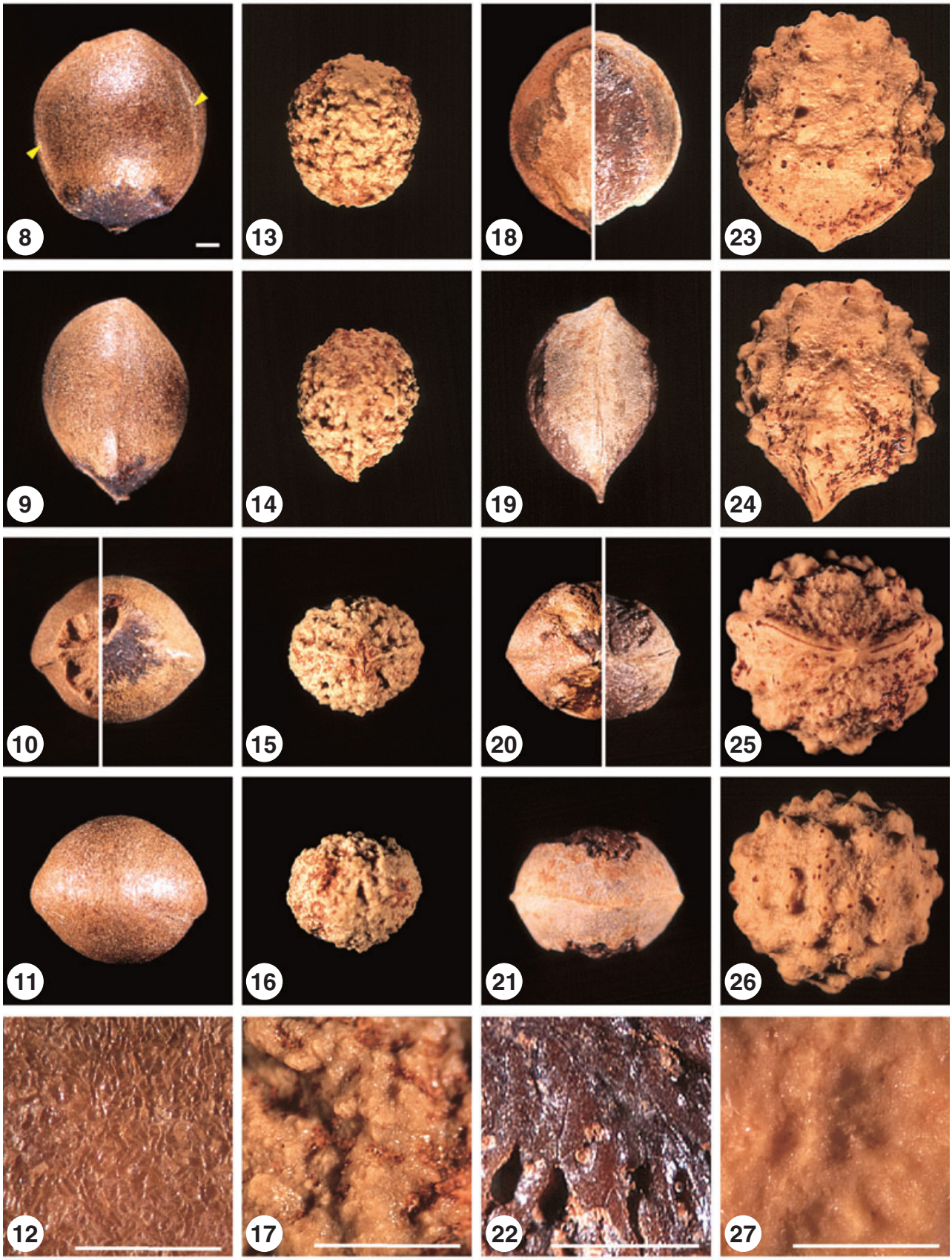

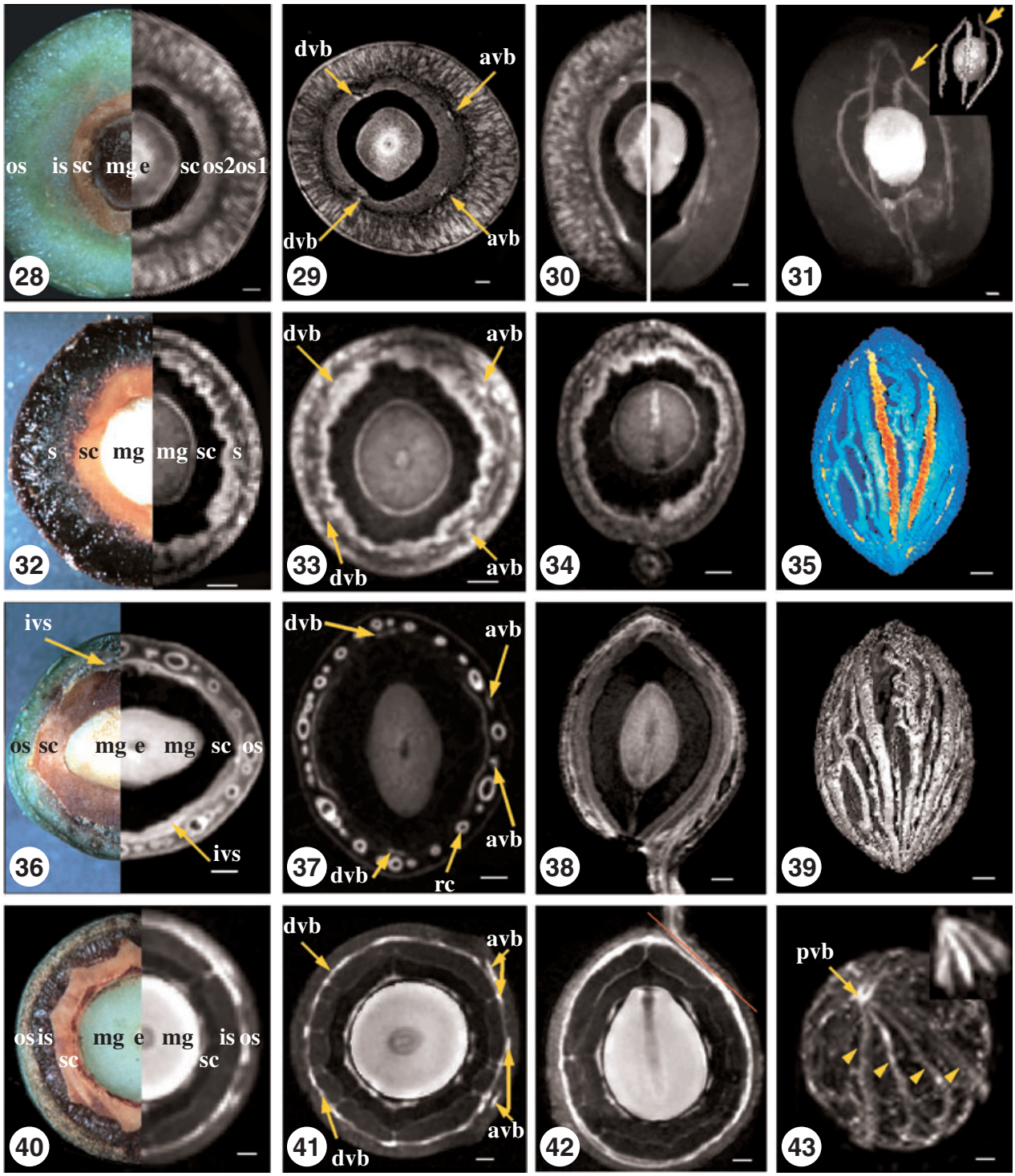

smoother surface of *P. andina* (cf. Figs 12, 17) and apparently lacking the internal chambered structure of that species. A beak-like protuberance at the micropylar end contained the micropylar canal (Fig. 14). Two narrow transverse ridges were present in the equatorial region and converged on the micropyle (Fig. 15).

At first glance, the NMR images of *P. taxifolia* (Figs 32–34) were similar to those of *P. andina*; both species have similar megagametophytes. In

Figures 28–43. Anatomical and NMR images of seeds of *Prumnopitys* spp. and *Afrocarpus falcatus*. Figs 28–31. *Prumnopitys andina*. Fig. 28. Composite image of median transverse slice, left side photographic image; right side T_2-weighted NMR image, voxel size $(164\ \mu m)^3$. Fig. 29. Median transverse NMR slice, T_2-weighted, voxel size $35 \times 35 \times 500\ \mu m$. Fig. 30. Median longitudinal NMR slice, left side T_2-weighted, right side T_1-weighted, voxel size $(164\ \mu m)^3$. Fig. 31. Maximum intensity projection of 3D T_1-weighted dataset. Inset: same dataset surface rendered; arrows indicate bifurcations of ascending vascular bundles. Figs 32–34. *Prumnopitys taxifolia*. Fig. 32. Composite image of median transverse slice, left side photographic image; right side T_1-weighted NMR image, voxel size $(94\ \mu m)^3$. Fig. 33. Median transverse NMR slice, T_1-weighted, voxel size $(94\ \mu m)^3$. Fig. 34. Median longitudinal NMR slice, T_1-weighted, voxel size $(94\ \mu m)^3$. Figs 35–39. *Prumnopitys ferruginea*. Fig. 35. Surface-rendered NMR image, T_2-weighted in false colour with vascular bundles highlighted. Fig. 36. Composite image of median transverse slice, left side photographic image; right side T_1-weighted NMR image, voxel size $(94\ \mu m)^3$. Fig. 37. Median transverse NMR slice, T_2-weighted, voxel size $(94\ \mu m)^3$. Fig. 38. Median longitudinal NMR slice, unweighted, voxel size $62.5 \times 62.5 \times 500\ \mu m$. Fig. 39. Surface-rendered NMR image, T_2-weighted. Figs 40–43. *Afrocarpus falcatus*. Fig. 40. Composite image of median transverse slice, left side photographic image; right side T_1-weighted NMR image, voxel size $(195\ \mu m)^3$. Fig. 41. Median transverse NMR slice, unweighted, voxel size $97 \times 97 \times 500\ \mu m$. Fig. 42. Median longitudinal NMR slice, unweighted, voxel size $94 \times 94 \times 500\ \mu m$. Fig. 43. Maximum intensity projection of T_2-weighted 3D NMR dataset, TE 30 ms, TR 500 ms, voxel size $(195\ \mu m)^3$; arrowheads indicate four ascending vascular bundles. Inset: horizontal slice, from same dataset, through the fertile complex which was at an angle of 20° to the vertical. avb – ascending vascular bundle, c – canal, dvb – descending vascular bundle, e – embryo, is – inner sarcotesta layer, ivs – inner, vestigial sarcotesta layer, mg – megagametophyte, os – outer sarcotesta layer, pvb – peduncular vascular bundle, s – sarcotesta, sc – sclerotesta. All scale bars = 1 mm.

P. taxifolia, however, the sarcotesta appeared divided into three zones, with irregular boundaries, which roughly corresponded with observed histological layers (Figs 51, 52, 74). In contrast to *P. andina*, the NMR images had a broad, relatively bright, peripheral zone; this corresponded to the epidermis, the three hypodermal layers as well as part of the outer sarcotesta (Fig. 74, zone 1/layers 1, 2 and 3 in part). Histological studies showed that the epidermal cells were elongated in the tangential plane and the hypodermal layers consisted of densely packed thick-walled rectangular cells typical of collenchyma (Fig. 53). The NMR images of the remainder of the sarcotesta appeared to differentiate a darker outer zone and a brighter inner zone (Figs 33, 34). Histological studies revealed that the outer layer consisted of large, loosely spaced, thin-walled, polygonal parenchymatous cells (Fig. 74 layer 3), whereas the inner one consisted of more densely packed, smaller cells of a similar type (Figs 52, 74 layer 4). In NMR images, the sclerotesta appeared more irregular in shape (Figs 33, 34) compared with *P. andina*. It was composed of densely packed sclerenchyma cells (Figs 54, 74 layer 5). Some isolated cells, whose detached membranes stained darkly with safranin/fast green, were scattered throughout the sarcotesta. These cells were probably tannin-rich.

In NMR images the positions of vascular traces were difficult to discern (Fig. 33, arrows), not only because of the lower contrast between them and the surrounding tissue, but also because of the heterogeneous pattern in the darker zone, approximately in the middle of which they were located (Figs 33, 74, 78). Their courses were most easily followed by using frame-by-frame analyses of 3D data sets (www.blackwellpublishing.com/products/journals/suppmat/BOJ/BOJ289/BOJ289sm.htm), and appeared similar to those of *P. andina*, with two ascending and two descending strands more or less equidistant from the sclerotesta (Fig. 78).

The main difference between the two species was in the number and extent of the resin canals. In *P. taxifolia* there were three resin canals in the middle of the outer sarcotesta layer, at the base of the fertile complex (Fig. 51); the central canal of the three was present only at the base of the fertile complex, whereas the remaining two each remained closely associated with a vascular strand (Fig. 56). The resin canals were lined with a layer of secretory cells (Fig. 57).

In this species, starch grains were ellipsoidal (*c*. 5 μm) and were present only in a semicircle of parenchyma cells around each vascular trace and the associated resin canal (Fig. 55).

PRUMNOPITYS FERRUGINEA

Fertile complexes of *Prumnopitys ferruginea* were ellipsoidal, with a very pronounced chalazal knob (Fig. 3). The example measured was 18×13 mm (excluding knob).

In size and shape the kernel of this species was similar to that of *P. andina*. It measured 8.5 mm long × 8 mm wide (major plane) × 6 mm thick (minor plane) (Figs 18–21). However, on both the abaxial and the adaxial sides there was a lobed depression in the central area of the sclerotesta (Figs 18, 20) that corresponded to the position of a vestigial inner sarcotesta layer revealed by histology (see below). The surface within these depressions appeared darker brown and

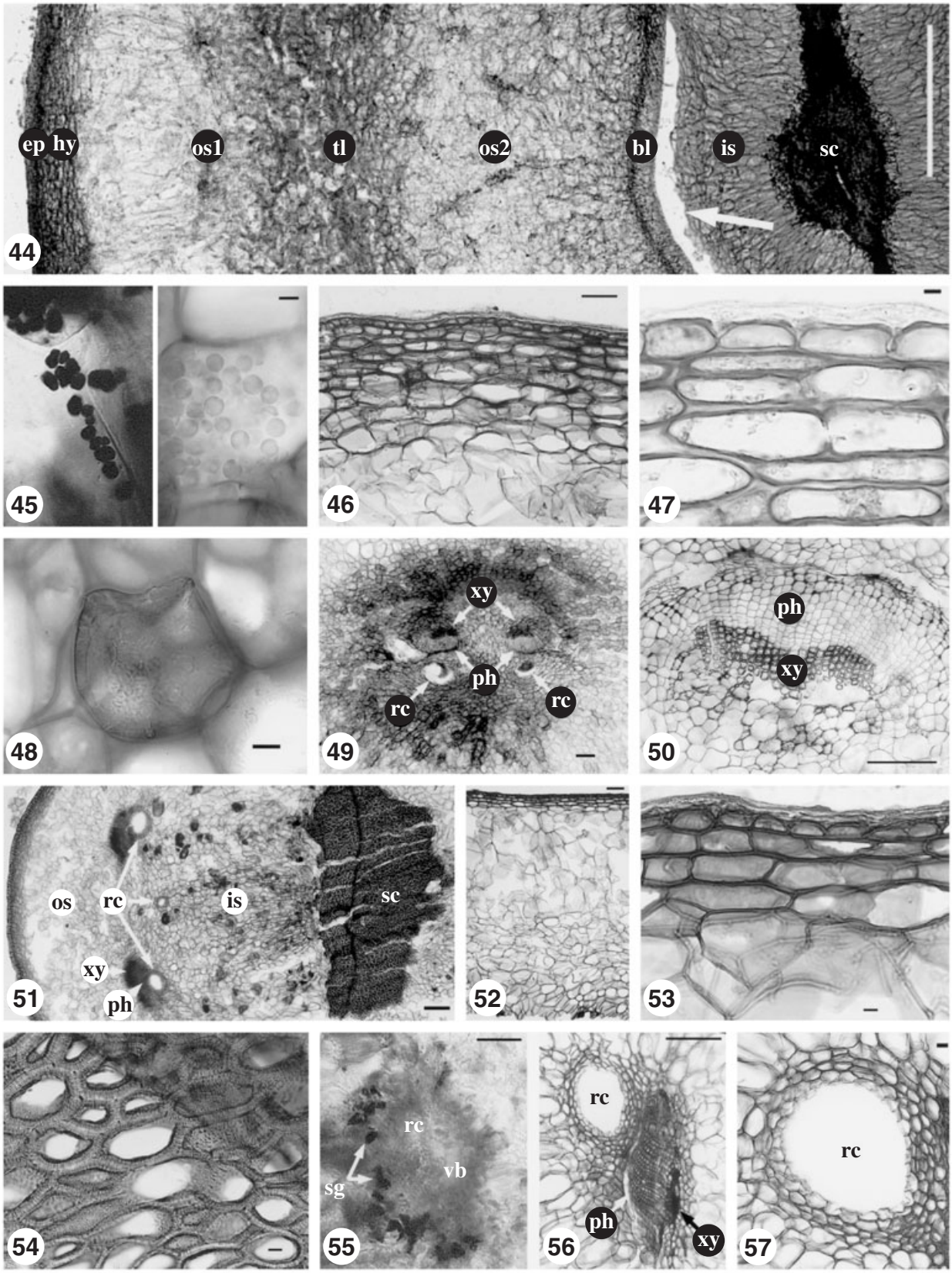

Figures 44–57. Histological sections of fertile complexes of *Prumnopitys andina* and *Prumnopitys taxifolia*. Fig. 44. *Prumnopitys andina*. Transverse section through base of fertile complex. Arrow indicates fracturing due to sectioning. Scale bar = 1 mm. Fig. 45. *Prumnopitys andina*. Starch grains in cells of outer sarcotesta layer (left, stained with iodine; right, unstained). Scale bar for both images = 10 μm. Fig. 46. *Prumnopitys andina*. Transverse section through outer sarcotesta layer, showing epidermis, hypodermis and outer sarcotesta cells. Scale bar = 100 μm. Fig. 47. *Prumnopitys andina*. Epidermis and hypodermis. Scale bar = 10 μm. Fig. 48. *Prumnopitys andina*. Cell with possible tannin deposits. Scale bar = 10 μm. Fig. 49. *Prumnopitys andina*. Section through vascular bundle region at the base of fertile complexes showing two vascular strands and vestigial resin canals. Scale bar = 100 μm. Fig. 50. *Prumnopitys andina*. Close-up of vascular bundle, near the sclerotesta; note absence of any associated resin canal (cf. Fig. 49). Scale bar = 100 μm. Fig. 51. *Prumnopitys taxifolia*. Transverse section through base of fertile complex. Scale bar = 100 μm. Fig. 52. *Prumnopitys taxifolia*. Section through outer sarcotesta layer. Scale bar = 100 μm. Fig. 53. *Prumnopitys taxifolia*. Close-up of epidermis and hypodermis. Scale bar = 10 μm. Fig. 54. *Prumnopitys taxifolia*. Section of sclerotesta. Scale bar = 10 μm. Fig. 55. Starch grains in cells located in a semicircle around a vascular trace. Scale bar = 100 μm. Fig. 56. *Prumnopitys taxifolia*. Vascular bundle with associated resin canal. Scale bar = 100 μm. Fig. 57. *Prumnopitys taxifolia*. Close-up of resin canal showing secretory cells. Scale bar = 10 μm. bl – boundary layer, ep – epidermis, hy – hypodermis, is – inner sarcotesta layer, os – outer sarcotesta layer, ph – phloem, rc – resin canal, sc – sclerotesta, tl – transition layer, xy – xylem.

smoother than the rest of the kernel (Fig. 22). The micropylar canal formed a long conical extension (Fig. 19). A narrow ridge encircled the equator of the kernel (Figs 19–21).

The internal structure of the sarcotesta in *P. ferruginea* was more elaborate than either *P. andina* or *P. taxifolia* (Figs 36–38, 75). Although the NMR images of the megagametophyte and sclerotesta appeared similar to those of the previous two species, the images of the sarcotesta revealed major differences: 2D slices showed two semicircular bright 'crescents' surrounding the sclerotesta (Figs 36, 37). These were composed of voluminous thin-walled cells (Figs 58, 59), filled with starch grains which stained with iodine (Fig. 60), and were interpreted as a vestigial inner sarcotesta layer. In transverse section, this tissue was separated from the outer sarcotesta layer by two conspicuous single cell layers (Figs 59, 75), indistinguishable by NMR (Figs 37, 75 zone 3/layers 4 & 5); the walls of these two cell layers stained strongly with safranin/fast green (Fig. 59). The outer sarcotesta layer (Fig. 75 zone 2/layer 3) was composed of relatively small thin-walled polygonal parenchyma cells (Figs 58, 59). The bright peripheral zone differentiated in NMR images corresponded to 1–3 densely packed hypodermal layers and an epidermis with irregularly shaped isodiametric cells with a 10-μm-thick cuticle (Fig. 61).

Two-dimensional equatorial transverse and longitudinal NMR slices showed a complex pattern of vascular traces and resin canals in the outer sarcotesta layer (Figs 36–38, 58, 79). The vascular traces could be followed as less intense spots among the brighter rings which marked the position of the resin canals in T_2-weighted NMR images of the sarcotesta (Fig. 37, and www.blackwellpublishing.com/products/journals/suppmat/BOJ/BOJ289/BOJ289sm.htm). In equatorial transverse sections, the two ascending traces were visible close together in the middle of the outer sarcotesta layer (Figs 37, 79, avb). They descended between the outer sarcotesta layer and the sclerotesta at either end of the longer axis (Figs 37, 79 dvb). The anatomy of the vascular traces was unusual in that the phloem was partly enclosed by the xylem (i.e. the bundle is partially amphivasal) and the xylem appeared as loosely arranged interrupted aggregations of strands (Fig. 62).

Within the outer parenchymatous sarcotesta layer, a ring of resin canals of varying diameters was also embedded (Figs 58, 63), which appeared bright in T_2-weighted NMR images (Fig. 37) owing to the presence of a surrounding layer of densely packed thin-walled cells and a lining of secretory cells (Fig. 63). In surface-rendered NMR images the interconnectivity of the canal network was revealed (Figs 35, 39), as were the vascular traces. The courses of the canals and traces can be best analysed in 3D datasets (www.blackwellpublishing.com/products/journals/suppmat/BOJ/BOJ289/BOJ289sm.htm).

Starch grains in *P. ferruginea* were *c.* 10 μm and were located entirely within the vestigial inner sarcotesta layer. Although somewhat irregular, they did not have the faceted appearance of those found in *P. andina*.

Afrocarpus falcatus

Fertile complexes of *A. falcatus* were more or less spherical, and lacked a chalazal knob (Figs 4, 5). The example measured was 14 mm in diameter.

The kernel of *A. falcatus* was the largest among the taxa analysed, almost spherical, 11 mm long × 10 mm wide (major plane) × 9 mm thick (minor plane), light reddish brown and the most elaborately ornamented (Figs 23–26). Numerous protrusions were scattered all over the kernel; these had hollow centres (Fig. 27). Two lateral ridged fracture lines were present on either side of the micropylar canal and the micropylar end was beak-like (Figs 23–25).

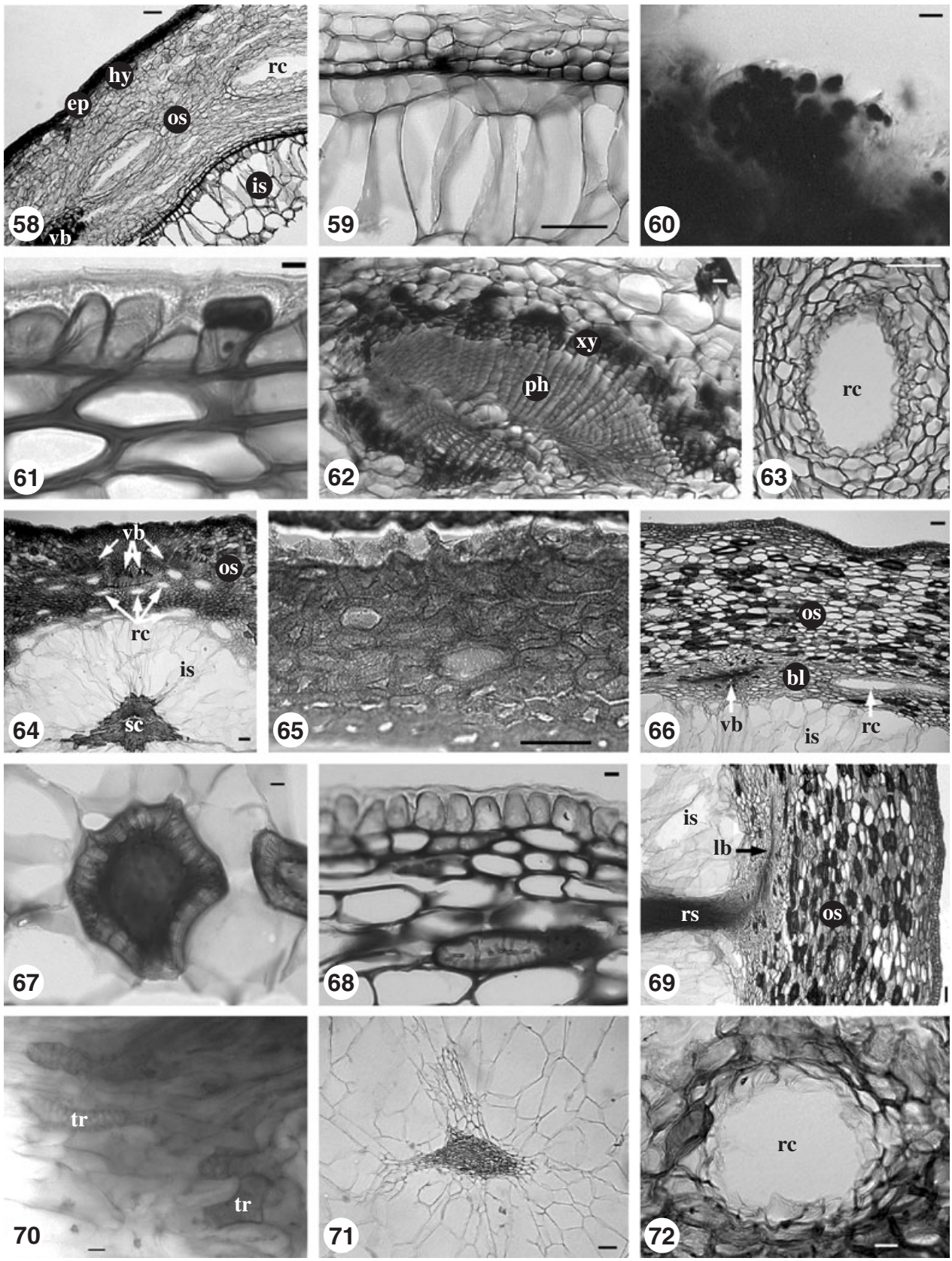

Figures 58–72. Histological sections of fertile complexes of *Prumnopitys ferruginea* and *Afrocarpus falcatus*. Fig. 58. *Prumnopitys ferruginea*. Transverse section through sarcotesta showing thick-celled boundary layers between the outer and inner sarcotesta layers. Scale bar = 100 μm. Fig. 59. *Prumnopitys ferruginea*. Close-up of thick-celled boundary layer. Scale bar = 100 μm. Fig. 60. *Prumnopitys ferruginea*. Starch grains in the vestigial inner sarcotesta layer. Scale bar = 10 μm. Fig. 61. *Prumnopitys ferruginea*. Epidermis and hypodermis. Scale bar = 10 μm. Fig. 62. *Prumnopitys ferruginea*. Vascular bundle with xylem partially enclosing the phloem. Scale bar = 10 μm. Fig. 63. *Prumnopitys ferruginea*. Resin canal showing secretory cells. Scale bar = 100 μm. Fig. 64. *Afrocarpus falcatus.* Transverse section through base of fertile complex showing the beginning of the sclerotesta at the micropylar end. The two median vascular bundles are still adjacent. Scale bar = 100 μm. Fig. 65. *Afrocarpus falcatus.* Section of sclerotesta. Scale bar = 100 μm. Fig. 66. *Afrocarpus falcatus*. Transverse section through sarcotesta showing numerous brachysclereids. Scale bar = 100 μm. Fig. 67. *Afrocarpus falcatus*. Close-up of brachysclereid showing radial pits. Scale bar = 10 μm. Fig. 68. *Afrocarpus falcatus*. Epidermis and hypodermis with brachysclereid. Scale bar = 10 μm. Fig. 69. *Afrocarpus falcatus*. Transverse section through sarcotesta, showing a lateral vascular bundle at the inner periphery of the outer sarcotesta and a radial vascular strand entering the inner sarcotesta. Scale bar = 100 μm. Fig. 70. *Afrocarpus falcatus*. Close-up of tracheids of radial vascular strand. Scale bar = 10 μm. Fig. 71. *Afrocarpus falcatus*. Transverse section through radial strand. Scale bar = 10 μm. Fig. 72. *Afrocarpus falcatus*. Resin canal showing secretory cells. Scale bar = 10 μm. ep – epidermis, hy – hypodermis, is – inner sarcotesta layer, lb – lateral bundle, os – outer sarcotesta layer, ph – phloem, rc – resin canal, rs – radial strands, sc – sclerotesta, tr – tracheid, vb – vascular bundle, xy – xylem.

Compared with unweighted NMR images (Figs 40–42), T_2-weighted ones (not shown here: see Glidewell *et al.*, 2002: fig. 1g–i) were darker and revealed less information overall. In contrast to *Prumnopitys*, the fertile complexes of *Afrocarpus* were much more radially symmetric in transverse sections (Figs 40, 41). As in the former, in equatorial transverse NMR images the embryo could be distinguished from the surrounding megagametophyte. Around the latter was a darker zone, corresponding to the endotesta, adjacent to which were bright triangular projections (Figs 41, 42). Whereas NMR images revealed four zones including the sclerotesta, histology differentiated six layers (Figs 41, 42, 64, 76). The outer surface of the sclerotesta (Fig. 76 zone 4/layer 6) was irregular due to the many conical protrusions (Figs 6, 23–26, 40). It appeared dark in NMR images due to the lack of mobile protons in the densely packed heavily sclerified cells (Fig. 65).

The inner sarcotesta layer (Fig. 76 zone 3/layer 5) was less intense than the outer sarcotesta in NMR images (Figs 41, 42), and consisted of radially elongated secretory cells (Figs 7, 64, 66). Gum exuded from cut surfaces (Fig. 5), its origin presumably in the inner sarcotesta. The outer sarcotesta layer [Fig. 76 zones 1 (excl. epidermis and hypodermis) & 2/layers 3 & 4] gave NMR images of intermediate intensity (Figs 41, 42), and consisted of densely packed thin-walled parenchymatous cells interspersed with numerous irregularly shaped brachysclereids (Figs 66–69) which contained many laminations and numerous branched radial pits (Fig. 67).

In NMR images the epidermis and the hypodermis layers could not be distinguished from the outer sarcotesta (Figs 41, 42). Histological sections revealed that the epidermis cells were isodiametric in transverse view with a thick cuticle extending deeply between the anticlinal walls and that the hypodermis consisted of one or two rows of thin-walled rectangular somewhat elongated cells (Fig. 68).

Four ascending vascular traces were located in the centre of the outer sarcotesta on the abaxial side of the fertile complex (Figs 41, 43, 64, 80). These arched over the chalazal end and from 3D NMR datasets (www.blackwellpublishing.com/products/journals/suppmat/BOJ/BOJ289/BOJ289sm.htm) it became obvious that they formed a branched system, with a variable number of descending traces (6–10, dependent on the number of bifurcations of the ascending traces and where the electronic 'slice' was made); these converged towards the micropylar end, all around the inner sarcotesta (Figs 41, 80). Of the four ascending traces, the two inner ones branched towards the chalazal end but the two outer ones did not. How the traces branched at the actual chalaza was difficult to interpret by NMR imaging due to lack of data in that region. Lateral traces branched off from the descending traces into the boundary between the outer and inner layers of the sarcotesta (Fig. 69). From these lateral traces, vascular strands extended radially through the inner layer of the sarcotesta (Figs 69, 71; tracheids are shown in close-up in Fig. 70) and then through the sclerotesta as far as its boundary with the endotesta, where they appeared to branch further (Fig. 6). Both photography (Fig. 6) and NMR imaging indicated that these radial strands terminated close to, but apparently did not enter, the megagametophyte.

In NMR images, the boundary zone (Fig. 76 NMR zone 2) between the outer and inner regions of the sarcotesta appeared bright (Fig. 41) due to the presence of these systems of vascular bundles and resin pockets, as verified by histology (Fig. 66). The resin pockets can be separately visualized using surface-rendered 3D data

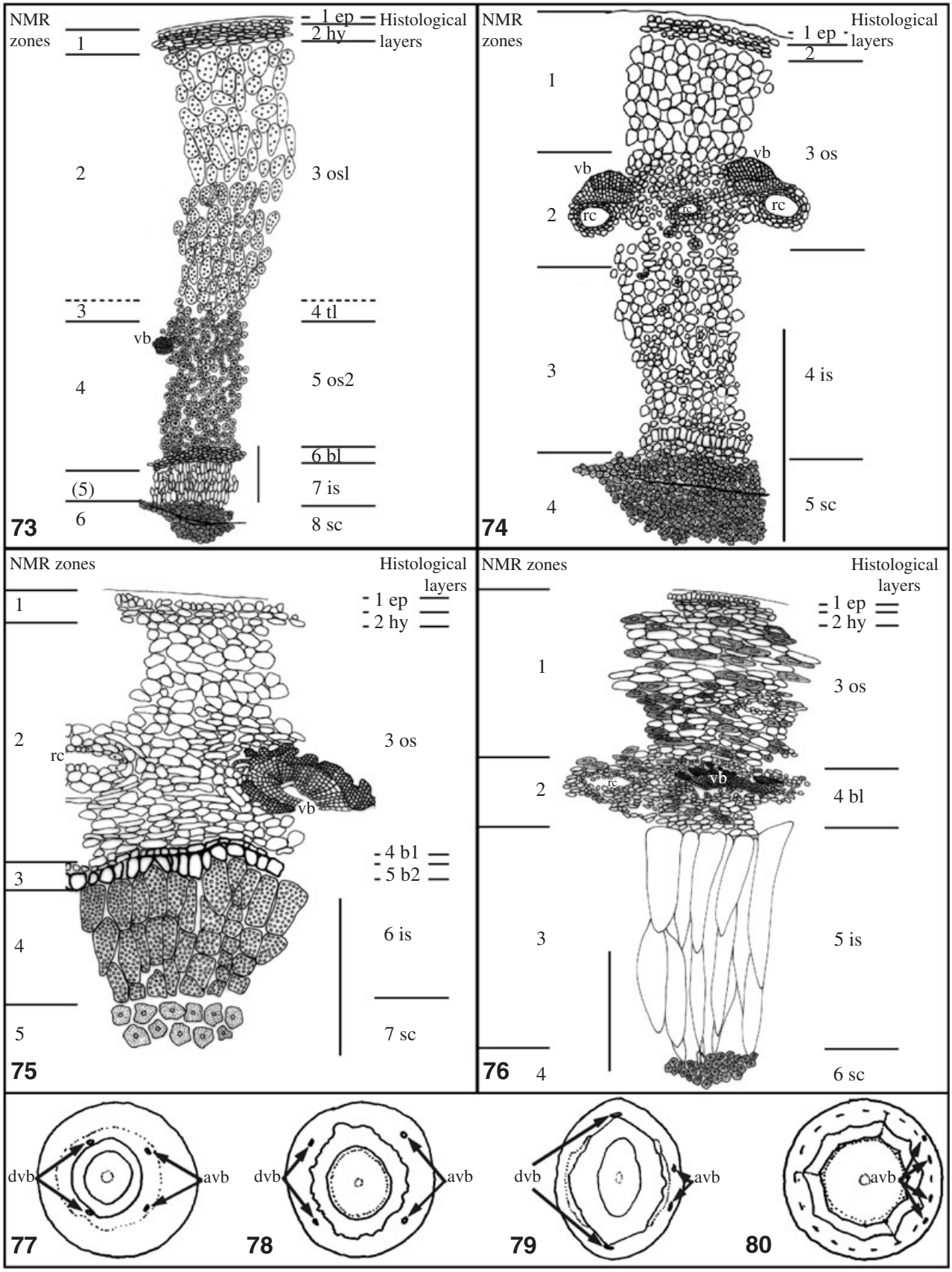

Figures 73–80. Drawings of the layer structure (Figs 73–76) and transverse section diagrams of positions of vascular bundles (Figs 77–80) of fertile complexes of *Prumnopitys* spp. and *Afrocarpus falcatus*. Figs 73, 77. *Prumnopitys andina*. Figs 74, 78. *Prumnopitys taxifolia*. Figs 75, 79. *Prumnopitys ferruginea*. Figs 76, 80. *Afrocarpus falcatus*. Figs 73, 74 – scale bar = 1 mm; Figs 75, 76 – scale bar = 500 μm. avb – ascending vascular bundle, bl, b1, b2 – boundary layer(s), dvb – descending vascular bundle, ep – epidermis, hy – hypodermis, is – inner sarcotesta layer, os – outer sarcotesta layer(s), rc – resin canal, sc – sclerotesta, tl – transition layer, vb – vascular bundle.

sets (www.blackwellpublishing.com/products/journals/suppmat/BOJ/BOJ289/BOJ289sm.htm). The entire secretory system consisted not only of the larger transversely elongated branched pockets in the boundary zone, but also of smaller, isolated, sometimes branched, ducts and pockets in the middle of the outer sarcotesta layer (Fig. 66). Both systems of resin pockets possessed several layers of densely packed cells and an inner ring of smaller thin-walled secretory cells (Fig. 72).

Starch grains were not seen in any cell layer in this species.

DISCUSSION

Previous anatomical studies of podocarpaceous fertile complexes have been relatively few and have usually lacked detail. This is particularly true where histology is concerned, as most papers have focused on vasculature; in comparison with the leaves, which have been extensively studied, the histology of the female reproductive structures of Podocarpaceae seems very poorly known and would repay study. Sinnott (1913) was one of the first to give a detailed general survey of the family, in which he studied several species belonging to what are now regarded as the genera *Dacrycarpus*, *Dacrydium*, *Halocarpus*, *Phyllocladus*, *Podocarpus* and *Prumnopitys*, and provided simple diagrams of vascular systems and internal tissue organization. At about the same time, Gibbs (1912) carried out a histological survey of 13 species belonging to what were then treated as four sections of *Podocarpus* (now the genera *Dacrycarpus*, *Podocarpus*, *Prumnopitys* and *Retrophyllum*). These included two of the three species of *Prumnopitys* studied by us (*P. ferruginea* and *P. taxifolia*), but not *P. andina* nor *Afrocarpus*. However, all her material was collected as very young stages (mostly pollination or prefertilization) and so, interesting as they are, her histological data cannot be directly compared with the much more mature stages used in this study. She noted the presence of starch cells in regions where we did not observe any, such as the apex of what she termed the nucellus in both *P. taxifolia* and *P. ferruginea*. The papers by Florin (1951, 1954) did not significantly advance earlier knowledge, at least concerning the Podocarpaceae. Studies of the vasculature of single species of *Prumnopitys* and *Afrocarpus* have been undertaken by Morvan (1983: *P. taxifolia*, as *Stachycarpus spicata* (R.Br.) Tiegh.) and Konar & Oberoi (1969: *A. gracilior*, as *Podocarpus gracilior* Pilg.), whereas Brooks & Stiles (1910) studied *Podocarpus spinulosus* (Sm.) R. Br. ex Mirb. and Jain (1978) examined *Podocarpus neriifolius* D. Don. More recently, Bobrov and co-workers have studied carpological characters of various podocarp genera (e.g. Bobrov & Karpun, 1995; Bobrov, 1996a,b; Bobrov & Romanov, 1999, *Sundacarpus*; Melikian & Bobrov, 1997, *Prumnopitys*, *Sundacarpus*, etc.). Most of this Russian work (other than the last cited paper) has only been reported briefly, often in conference proceedings that are rarely available outside Russia. It culminated in a paper by Melikian & Bobrov (2000), which used the carpological characters studied by them as the basis for a radically new classification of *Podocarpaceae*, dividing the family into a large number of smaller (often monogeneric) ones that were split between seven orders (several new), and erecting several new genera. Tarbaeva (1997) studied the ultrastructure of the 'seed coat' of six genera of podocarps but, of the taxa she studied, only *Prumnopitys ferruginea* was also studied by us. Meanwhile, the female fertile complexes of *Acmopyle pancheri* have recently been studied by Mill *et al*. (2001), employing a mixture of NMR imaging and conventional histology as in the present study. The lack of detailed studies is partly due to scarcity of available material outside the southern hemisphere and partly because, even when material is in cultivation, it produces cones rarely, if at all (*Acmopyle* at RBGE being a notable exception: Mill *et al*., 2001). No doubt the difficulties encountered in sectioning mature or nearly mature material have also been a factor; most published studies have been based on young ovules that we assume did not possess the extremely hard, thick sclerotesta that develops during the resting phase (Mill *et al*., 2001).

When previous studies have been sufficiently detailed, such as those of Morvan (1983) for *Prumnopitys taxifolia* and Jain (1978) for *Podocarpus neriifolius*, they reveal certain variations on a common theme. An ascending vascular supply rises to a more or less well-developed terminal chalazal knob (misleadingly termed the 'apical knob' by Sinnott, 1913), which Gibbs (1912) and Sahni & Mitra (1927) regarded as homologous with the distal end of the ovuliferous scale. This may well be a correct interpretation but the structure is also remarkably similar to the organization of the ovule of *Anasperma burnense* A.

Long (Long, 1966), an Early Carboniferous hydrasperman gymnosperm. This had an (apparently) inverted ovule with a prominent chalazal knob, from which a structure that Long termed a raphe extended back alongside the ovule to attach it to the cupule in which it was borne; this so-called raphe appears to serve the same function as both the ovuliferous scale of typical conifers and the epimatium of podocarps. However, without considerable research it would be difficult to establish whether this is evidence of any homology between the respective structures.

From the chalazal knob the vascular traces then descend, in some species branching repeatedly in a complex manner as they do so. *Afrocarpus* seems to be an exception to this pattern: Konar & Oberoi (1969) mentioned no chalazal knob in *A. gracilior*, and described a system in which, as the vascular traces ascend, each of them "gives out small branches toward the inner part of the ovule", but neither the significance of these, nor their actual course, was elaborated in their paper. In all previous studies, authors have recorded the presence of a more or less developed system of resin or tannin ducts or canals associated in various ways with the vascular bundles in *Afrocarpus* and *Prumnopitys* but have given few or no details regarding the nature of the secretory systems.

Complementarity of techniques

NMR imaging is indispensable in obtaining a complete understanding of the three-dimensional (3D) organization of vascular and secretory systems in a way that has not been possible, even with serial histological sections. It is also a powerful tool with which to study complex tissue organizations as found in *Afrocarpus* and *Prumnopitys* (particularly *P. ferruginea*). A detailed interpretation of the structures and tissue zones revealed by NMR imaging in the fertile complexes of *P. ferruginea* and *A. falcatus* was given by Glidewell *et al*. (2002). Conventional histology often showed that the system of tissue layers was more complex than the zones discriminated by NMR imaging. Sometimes the latter did not correspond exactly with the actual tissue layers (Figs 73–76). However, NMR can also discriminate between tissue zones that are not apparent in a thin section, as in *P. taxifolia* (Fig. 74), and careful interpretation is necessary. Moreover, the weighting regime used to capture the images often influences such discrimination, as discussed by Glidewell *et al*. (2002). These authors found that, for *Prumnopitys* and *Afrocarpus*, a weighting regime with some T_1 as well as T_2 weighting was the most likely to produce discriminative images. For selective 3D imaging of resin canals, T_2 weighting gave the most striking images (Figs 35, 39) but vascular bundles in *P. andina* were best revealed in maximum intensity projections of T_1-weighted datasets (Fig. 31). In the specimens of that species, tissue variation in the sarcotesta was best revealed with T_2 weighting, whereas T_1-weighted images of that tissue had a more uniform appearance with which the vascular traces gave good contrast for maximum intensity projection. Maximum information of potential taxonomic use is therefore obtained from a combination of NMR imaging and conventional histology, as employed here and by Mill *et al*. (2001) and Glidewell *et al*. (2002). Relaxation weighting regimes were chosen in order to extract the maximum amount of anatomical information from the NMR data sets, and judicious comparison of images acquired with different weighting regimes (or direct generation of relaxation-time maps) can provide additional information as to the nature of the tissue imaged.

In all four species examined, we found it impossible to differentiate the epimatium tissue from that of the seed proper, either in NMR images or in frozen sections. At the stages we studied, the epimatium and integument are fused in all species. However, had younger stages been used, differentiation of the epimatium might have been possible. Previous workers such as Morvan (1983) have equated the entire region that we studied, from epidermis to the outer boundary of the sclerotesta, with the epimatium. Our previous work with *Acmopyle* (Mill *et al*., 2001) suggests that, in that genus at least, this is unlikely and that only some of this tissue in *Acmopyle* is derived from the epimatium, the remainder being derived from the ovule. However, Tomlinson (1992: fig. 62) illustrated a very young stage of *Prumnopitys ferruginea* in which the ovule was already more or less enveloped by the epimatium; thus, it is indeed possible that all the tissue we studied was epimatial in origin.

Differences between *Prumnopitys* and *Afrocarpus*

All three species of *Prumnopitys* studied were found to differ from *Afrocarpus* in several important details. The exterior of the sclerotesta in all the *Prumnopitys* species examined (including *P. taxifolia*) lacked the conical protuberances characteristic of *Afrocarpus* and which is an autapomorphic character for that genus, being found in all species (Konar & Oberoi, 1969; Gaussen, 1974) but not (so far as is known) in any other genus of Podocarpaceae, including *Nageia* and *Retrophyllum*, the two nearest relatives of *Afrocarpus* as inferred from recent molecular phylogenetic data (Conran *et al*., 2000; Sinclair *et al*., 2002).

Tissue organization in all four species was broadly similar, with a tripartite division of the regions studied into (i) epidermis and hypodermal layers, (ii) outer sarcotesta proper and (iii) sclerotesta. The presence of

what we interpreted as hypodermal layers in all species was significant and in marked contrast to the foliage of the same taxa, because numerous authors have noted the total absence of hypodermis in the leaves of all species of *Prumnopitys* as well as *Sundacarpus* (e.g. Orr, 1944; Gray & Buchholz, 1951a, b; Gaussen, 1974). *Afrocarpus* does have hypodermis in the leaves of all species (Orr, 1944; Gray, 1953; Konar & Oberoi, 1969) but it is fibrous, discontinuous in small groups, and unlike the continuous layers of subepidermal cells interpreted by us as hypodermis in its cones.

There were major differences in the vasculature systems. In *Prumnopitys*, two strands ascend to the chalazal knob and then branch and descend, but in *Afrocarpus* between three and five strands (Konar & Oberoi, 1969, *A. gracilior*) ascend to the chalazal end, where (as in *Nageia*) there is no knob. We observed four ascending strands in our material of *A. falcatus* and noted that the point of divergence of these traces at the proximal end varied between individual fertile complexes; in some they diverged as soon as they entered the complex from the peduncle, whereas in others they diverged further up, within the complex. This may in part account for the variation in strand number reported by Konar & Oberoi (1969). Bobrov & Romanov (1999), in a very brief, unillustrated report, stated that eight bundles were present in *Afrocarpus* but this does not agree with our observations, where a total of at least ten and sometimes up to 14 traces could be discerned in maximum intensity NMR datasets, the number varying and dependent on the number of bifurcations of the descending traces. Konar & Oberoi (1969) stated that, in *A. gracilior*, all the bundles extend 'upwards' [meaning downwards, because ovule inversion was not taken into account] to the chalaza where the median strand bends over the [topographical] 'top' [morphologically, the base, due to inversion'] of the ovule and may divide into two or more strands, whereas the lateral bundles 'descend' [i.e. ascend] towards the micropyle, branching laterally and inwards as they do so. We were able to verify, and clarify to some extent, the branching pattern of these lateral strands but not how the bundles bend over the chalaza.

A system of radial vascular strands penetrating the sclerotesta is present in *Afrocarpus*, but absent in *Prumnopitys*. This arrangement seems to be unique in the Podocarpaceae and possibly in the extant gymnosperms as a whole. Its nature was briefly described by Konar & Oberoi (1969), including the existence of transverse strands, but they offered no discussion of its significance. The work reported by Glidewell *et al*. (2002) and in the present paper (which corrects some interpretations reported in that paper) has for the first time shown that there is a complex network of transverse vascular traces that originate in the outer boundary layer of the sarcotesta, as radial protrusions from the tangential system of traces in that layer, and pass through the gum-secreting inner sarcotesta to enter the kernel via the conical protuberances of the sclerotesta. Each protuberance has a small distal hole (visible to the naked eye) through which the strand passes. At the inner end of the protuberance, further short branches can sometimes be seen close to the endotesta (Fig. 6) although the significance of these is still obscure. Some extinct cordaites, such as *Cardiocarpus spinatus* Roy Graham (Andrews & Felix, 1952), also had a thick, 'spinose' sclerotesta whose protuberances extended into the adjacent sarcotesta in a similar manner to *Afrocarpus*. The ovules of cardiocarpalean coniferophytes in general were characterized by their double vascular system, with both the integument and the base of the nucellus vascularized (Hilton, Wang & Tian, 2003, and references therein). Among living gymnosperms, only the cycads have both an integumental and a nucellar vascular system (Stevenson, 1990). All conifers have only the integument (including epimatium when present, as in most Podocarpaceae) vascularized (Tomlinson & Takaso, 2003). The significance of the peculiar vascularization of *Afrocarpus*, which shows intriguing tendencies towards an as yet unproven double system, needs further study.

Numerous brachysclereids occur in the outer sarcotesta layer of *Afrocarpus* but are absent in all three species of *Prumnopitys* studied. This mirrors the distribution of sclereids in the foliage, because they are also absent in the leaves of the same three species of *Prumnopitys* but present in all species of *Afrocarpus* (Gaussen, 1974). The sclereids in the sarcotesta of *Afrocarpus* are similar in appearance to those found in *Juniperus* of the Cupressaceae as illustrated by Napp-Zinn (1966: fig. 53).

There is a single system of resin ducts in *Prumnopitys*, whereas in *Afrocarpus* there were three apparently independent systems: two systems of branched pocket-like chambers in the outer sarcotesta layer and the boundary layer, and a system of elongated cells forming the inner sarcotesta layer and producing gum. *Afrocarpus* and *Prumnopitys* also differ markedly in the internal and external structures of their fertile complexes from those of *Podocarpus*, as can be seen when comparing the results obtained for two different species of *Podocarpus* (belonging to different subgenera) by Jain (1978: *P. neriifolius*) and Masson *et al*. (2001: *P. nivalis* Hook.) with those reported here and by Glidewell *et al*. (2002). The data therefore confirm the current view that *Afrocarpus* and *Prumnopitys* (as currently delimited) both deserve generic rank and should no longer be classified within *Podocarpus* as they were by Buchholz & Gray (1948a).

All three *Prumnopitys* species possessed starch grains in some cells, whereas these were not found in *Afrocarpus*. Starch grains were also not mentioned as occurring in *Afrocarpus* by Konar & Oberoi (1969).

Differences and similarities between *Prumnopitys* species

All three studied species of *Prumnopitys* had several unique characters found in none of the others (nor in *Afrocarpus*). *P. andina* and *P. taxifolia* were more similar to each other than either was to *P. ferruginea*. Characters shared by *P. andina* and *P. taxifolia* included epidermal cells elongated in the transverse plane (instead of irregularly isodiametric as in *P. ferruginea*) and a megagametophyte that is almost circular in transverse section, rather than markedly ellipsoidal as found in *P. ferruginea*. The distribution of resin canals was also similar, although in *P. andina* these appeared to be confined to the base of the fertile complex, whereas in *P. taxifolia* the duct system extended further into its sarcotesta. Both systems were relatively rudimentary when compared with the complicated branched network, consisting of many interconnected canals located in the outer sarcotesta, possessed by *P. ferruginea* and which gave such bright features in its NMR images. However, there were some significant differences between the fertile complexes of *P. andina* and *P. taxifolia*, both in their histology and in the NMR images obtained, that had been unexpected on the evidence from molecular phylogenies (Sinclair *et al*., 2002).

Sarcotesta tissue organization in the three species of *Prumnopitys* was unique to each. *P. andina* had more hypodermal cell layers (four to five) than *P. taxifolia* (three), and a much more complex organization of layers between the hypodermis and the sclerotesta; no fewer than seven principal histological layers could be discerned, compared with six in *P. ferruginea* and only four in *P. taxifolia*. This was principally due to the much more heterogeneous inner sarcotesta layer of *P. andina* compared with *P. taxifolia*. *P. ferruginea* was characterized by its very sharply defined, narrow boundary layer (two cells thick) between the outer and inner parts of the sarcotesta, and by the vestigial nature of the inner layer of the sarcotesta, which formed two saucer-shaped bodies (Figs 36, 37) in the equatorial region of the fertile complex. Using NMR imaging, these bodies had a longer T_2 relaxation time than the adjacent sarcotesta and sclerotesta zones, indicating the presence of closely packed water-rich cells. These 'saucers' perhaps correspond to the narrow strips on the abaxial and adaxial faces where the epimatium and integument in this species are not fused (Sinnott, 1913). The outer surface of the sclerotesta was also different in each species. Unexpectedly, *P. taxifolia* was found to have a highly ornamented sclerotesta surface, whereas those of *P. andina* and *P. ferruginea* were both nearly smooth, although in the latter species the vestigial inner sarcotesta left two marked depressions in the sclerotesta. The ornamentation explains the undulate outline of the NMR images of the sclerotesta in *P. taxifolia*. The two species with less sculptured sclerotesta surfaces (*P. andina* and *P. ferruginea*) nevertheless showed differences, such as the peculiar median lobes of *P. ferruginea*.

The two simplest vasculature/duct systems are those of *P. andina* and *P. taxifolia*, which were very similar to each other; those of *P. ferruginea* are far more complex and quite different from the other two. However, the remaining species of *Prumnopitys* should be studied before definite conclusions are drawn concerning homologies between tissue layers or any evolutionary trends in sarcotesta tissue organization and vasculature. The partially amphivasal vascular bundles found in *P. ferruginea* were particularly noteworthy. Our observations confirm those of Sinnott (1913), who went further and said that in some cases the xylem completely encircled the phloem in *P. ferruginea*. Sinnott also noted a tendency towards amphivasal bundles in *P. taxifolia* but we did not observe this in our material and it could be that in *P. taxifolia* the amphivasal tendency is only present in very young material. Completely amphivasal bundles have hitherto been assumed to be unknown in gymnosperms and to be found only in certain monocots (Mauseth, 1988; Fahn, 1990; Zhong, Taylor & Ye, 1999). However, Brooks & Stiles (1910) noted that the descending bundles in the ovule of *Podocarpus spinulosus* showed a tendency towards amphivasal structure. Thus, such a tendency towards amphivasal bundles may be more widespread in Podocarpaceae, and thus in gymnosperms, than previously believed.

Each species examined possessed a characteristic type of starch grain, unique to it. Given that the three species are presently usually classified in the same genus, this was not expected. There seems to have been no study on the variation in starch grain morphology in the Podocarpaceae. However, it is known that in other groups, e.g. grasses, there is considerable variation between genera and that specific taxa can often be identified by their starch grain shape and form (Fahn, 1990; Wen & He, 1989, 1991; Thomasson, 1997). Such a study in Podocarpaceae would therefore seem worthwhile.

Systematic implications

De Laubenfels (1978) divided *Prumnopitys* into two sections. Sect. *Sundacarpus* (originally *Podocarpus* sect. *Sundacarpus*: Gray & Buchholz, 1951b) com-

prised only *P. amara*, which is now usually recognized as the separate genus *Sundacarpus* (Page, 1989, 1990; Farjon, 2001) although not everyone agrees (e.g. Kelch, 2002). Sect. *Prumnopitys* comprised the remaining nine species and was not further subdivided by de Laubenfels.

Gray & Buchholz (1951a) proposed *Podocarpus* sect. *Stachycarpus* subsect. *Idioblastus* for three Australasian species now regarded as *Prumnopitys ferruginoides* (New Caledonia; including *Podocarpus distichus* J. Buchholz) and *Prumnopitys ladei* (Queensland, Australia). The subsection was defined by Gray & Buchholz by the presence of idioblasts in the leaves; idioblasts were also reported as occurring sparingly in the leaves of *P. ferruginea* by Orr (1944) although Gray & Buchholz did not include that species in their subsect. *Idioblastus*. More recently, *P. ferruginoides* and *P. ladei* as well as *Podocarpus distichus* (i.e. *Podocarpus* subsect. *Idioblastus*) plus *P. ferruginea* were treated as the four species of *Stachypitys*, which Melikian & Bobrov (2000) separated from *Prumnopitys s.s.* on the basis of their single fertile complexes and various differences of the testa of the fertile complex. The genus was typified by *S. ferruginea* (G. Benn. ex D. Don) A.V. Bobrov & Melikian (= *Prumnopitys ferruginea*). We have found *P. ferruginea* to be very different from *P. andina* and *P. taxifolia* in its fertile complex characters (differently shaped, ellipsoidal megagametophyte; complex network of resin canals; different locations of the ascending and descending vascular strands in equatorial sections) and there might well be some justification in recognizing *Stachypitys*, particularly since Tomlinson (1992) has pointed out that *P. ferruginea* also differs from *P. taxifolia* in cone position (basal nodes of previous year's growth in *P. ferruginea*, distal on current year's growth in *P. taxifolia*; Tomlinson gave no details for *P. andina* but its female cones are also distal on the current year's growth: our unpublished observations). However, neither *P. ladei* nor *P. ferruginoides* were sampled by us and it is necessary to obtain comparable data for those species before a final judgement can be made. Conversely, between *P. andina* and *P. taxifolia* we observed differences (e.g. several extra sarcotesta layers in *P. andina*; irregularly sculptured sclerotesta of *P. taxifolia*) as well as similarities (presence of cell inclusions in both species; very similarly shaped megagametophytes, markedly different from that of *P. ferruginea*). If one embarks on taxonomic splitting along the lines of Melikian & Bobrov's work, perhaps *P. taxifolia* should be generically or infragenerically segregated too, rather than both it and *P. andina* retained in *Prumnopitys* even in a restricted sense. Data comparable to those presented here are lacking for the Central American species included in *Prumnopitys s.s.* by Melikian & Bobrov (2000) and it is therefore premature to offer an opinion. The tropical South American species complex (*Prumnopitys montana* and its allies) that was recently segregated as *Botryopitys* (= *Van-Tieghemia*, nom. illegit.) by Doweld (2001) and Melikian & Bobrov (2000) also requires morphological and anatomical study.

The data obtained in this study lend some support to the relationships within *Prumnopitys s.l.* (including *Sundacarpus*) inferred from molecular research by Sinclair *et al.* (2002). In the latter study, using nuclear internal transcribed spacer 2 (ITS2) and chloroplast *trn*L-F intron/spacer sequences, two subclades were recovered, one consisting of *P. andina* and *P. taxifolia* as sister taxa (plus *Sundacarpus* as sister to both), the other of *P. ladei* sister to *P. ferruginea* and *P. ferruginoides*. These correspond to *Prumnopitys s.s.* (plus *Sundacarpus*) and *Stachypitys*, respectively. The molecular phylogenetic results obtained by Conran *et al.* (2000; using chloroplast *rbc*L sequences) were less consistent with the observed carpological differences, because they obtained three small clades: (1) *P. andina* and *P. ferruginoides*, (2) *P. ferruginea* and *Sundacarpus* and (3) *P. ladei* and *P. taxifolia*. Thus, in their work, *Prumnopitys s.s.* was split across two clades and *Stachypitys* across all three. Kelch's (2002) study using 18S is the only one to have sampled any of the Central American species of *Prumnopitys s.s.* (*P. harmsiana* (Pilg.) de Laub.), but, although *Prumnopitys* including *Sundacarpus* was resolved as a monophyletic group, little else about intrageneric relationships can be inferred from his results. No molecular phylogenetic study to date has sampled the tropical American group that has been segregated as *Botryopitys*.

Bobrov & Romanov (1999) first suggested a close relationship between *Afrocarpus* and *Sundacarpus* based on perceived similarities in carpological characters. These included eight vascular traces in *Afrocarpus* and 16 (8×2) in *Sundacarpus*, the presence of what they termed 'lysigenous cavities' in the epimatium of both genera, and 'sclerenchymatous mesotesta and parenchymatous endotesta' (Bobrov & Romanov, 1999). They used these similarities to place the two genera in a very restricted Podocarpaceae that also included *Podocarpus* (*s.s.*) and *Margbensonia* (= *Podocarpus* subgen. *Foliolatus*) but no other genera. We have shown in this paper that *Afrocarpus* does not necessarily always have eight vascular traces. Indeed, when ascending and descending traces are reckoned together, the number we observed was always at least ten and sometimes approached the 16 observed in *Sundacarpus*. Thus, vascular trace number cannot be taken as such a clear-cut difference between *Afrocarpus* and *Sundacarpus* as Bobrov & Romanov made it out to be. Moreover, they made no mention of the radial vascular strands of *Afrocarpus* or whether a

similar system is present in *Sundacarpus*. Their reference to 'sclerenchymatous mesotesta' presumably simply refers to a sclerotesta and if so it is of no significance because virtually all podocarps develop a sclerotesta to some extent. Furthermore, their report of lysigenous cavities in *Afrocarpus* and *Sundacarpus* must be treated with great caution. Turner (1999) has suggested that most, if not all, literature reports of lysigenous cavities in plant tissues are due to artefacts of fixation, or misinterpretation of the cell morphology. We found no evidence of lysigeny in *Afrocarpus* (the ducts of both systems observed by us appeared to be schizogenous, as in *Prumnopitys*).

Molecular phylogenetic analyses (Conran *et al*., 2000; Kelch, 2002; Sinclair *et al*., 2002) suggest that *Sundacarpus* should be grouped within, or at least sister to, *Prumnopitys* (or part of it). None suggests any close phylogenetic relationship between *Sundacarpus* and *Afrocarpus*, which are consistently placed in different major clades within the family, *Afrocarpus* being consistently placed in a clade with *Nageia* and *Retrophyllum* that is far removed from the one containing *Prumnopitys*, *Lagarostrobos*, *Halocarpus*, *Parasitaxus*, etc. However, Melikian & Bobrov (2000) removed those two genera from Podocarpaceae and transferred them both to Nageiaceae, which they placed in Cephalotaxales, not Podocarpales. Therefore, any similarities between *Afrocarpus* and *Sundacarpus* observed by Bobrov & Romanov (1999), if they were found to hold, would appear to be examples of convergence. A similarly critical anatomical scrutiny of *Sundacarpus* fertile complexes (and also those of *Nageia* and *Retrophyllum*) using NMR imaging and histology would be an ideal method to test whether the inferences drawn from molecular phylogenetics are correct. If Bobrov and Romanov's observations were correct and *Sundacarpus* does have 16 vascular strands, that would perhaps be one major distinction between it and *Prumnopitys*, which only has two ascending strands per ovule; unfortunately Bobrov and Romanov's brief abstract did not distinguish between ascending and descending strands.

CONCLUSIONS

This study yielded some unexpected results. Each species of *Prumnopitys* investigated had its own distinctive carpological 'signature', extending even to unique starch grain morphologies, suggesting that further work needs to be done to clarify the relationships between the species conventionally classified in the genus (as by Farjon, 2001). *Afrocarpus* is very different, and its system of radial strands is unique and worthy of further investigation. The work has demonstrated that much conventional histological work still needs to be done on the remaining species of *Prumnopitys* (particularly their cones) and that this should be extended to the family in general. NMR imaging, when interpreted carefully alongside the histology, is extremely useful in clarifying the complexities of the internal structures in ways that cannot be achieved by histology alone, and can explore tissues that cannot be studied by histological methods because of their extreme hardness. Further studies along the lines of the one reported here will greatly help in our understanding of this relatively poorly known family of conifers.

ACKNOWLEDGEMENTS

Joshua Salter (Auckland, New Zealand) kindly sent several batches of cones of *Prumnopitys ferruginea* and *P. taxifolia* from localities in New Zealand. Antonia Eastwood (until recently a PhD student at the Institute of Cell and Molecular Biology, University of Edinburgh) collected cones of *Afrocarpus falcatus* from a plantation on St. Helena. We thank Mary Mendum for the excellent drawings. The Royal Botanic Garden Edinburgh (RBGE) and the Scottish Crop Research Institute (SCRI) are supported by the Scottish Executive Environment and Rural Affairs Department (SEERAD). This paper is a product of RBGE Project FFL/99/060, funded by the Flexible Fund of SEERAD. The NMR imager at SCRI was purchased by Mylnefield Research Services Ltd.

SUPPLEMENTARY MATERIAL

The following material is available from:
www.blackwellpublishing.com/products/journals/suppmat/BOJ/BOJ289/BOJ289sm.htm

Appendix S1. Comparative anatomy and morphology of fertile complexes of *Prumnopitys* and *Afrocarpus* species (Podocarpaceae) as revealed by histology and NMR imaging, and their relevance to systematics.

REFERENCES

Andrews HN, Felix CJ. 1952. The gametophyte of *Cardiocarpus spinatus* Graham. *Annals of the Missouri Botanical Garden* **39:** 127–135.

Arber A. 1910. On the structure of the Palaeozoic seed *Mitrospermum compressum* (Will.). *Annals of Botany* **24:** 491–509 & plates XXXVII–XXXIX.

Bobrov AVFCh. 1996a. Korrelyatsiya mezhdy stroennem semennoj kozhury i sposobami disseminyetsii u nekotorykh predstavitelej podyaka *Podocarpales* (Pinophyta). [Correlation between seed coat structure and means of dissemination of some representatives of order *Podocarpales* (Pinophyta).] In: *Proceedings of Symposium Reproductive Biology of Plants, Per'm*: 60–62. [In Russian.]

Bobrov AVFCh. 1996b. Bitegmal'nie semena predstavitelej podyadkov Podocarpales, Cephalotaxales i Taxales. [Bitegmic seeds of representatives of orders Podocarpales, Cephalotaxales and Taxales.] *Proceedings of IX International Congress on Plant Phylogeny* **1996C:** 23–26.

Bobrov AVFCh, Karpun UN. 1995. *Semeistvo nogoplodnikovie ili podokarpovie Podocarpaceae Endlicher 1847. [Results and perspectives of introduction of woody plants in Russia, No. 3.]* Sotchi: 'Belyie Notchi' Botanic Garden.

Bobrov AVFCh, Romanov MS. 1999. Seed coat structure and systematic relationships of *Sundacarpus amara* (Blume) C.N. Page (Podocarpaceae (Dumort.) Endl. s.l.). In Manitz H, Hellwig FH, eds. *14. Symposium Biodiversität und Evolutionsbiologie. Zusammenfassungen der Vorträge und Poster Teilhehmerliste*. Jena: Institut für Spezielle Botanik der Friedrich-Schiller-Universität, 20.

Brooks FT, Stiles W. 1910. The structure of *Podocarpus spinulosus*, (Smith) R.Br. *Annals of Botany (Oxford)* **24:** 305–318.

Buchholz JT, Gray NE. 1948a. A taxonomic revision of *Podocarpus*. I. The sections of the genus and their subdivisions with special reference to leaf anatomy. *Journal of the Arnold Arboretum of Harvard University* **29:** 49–63.

Buchholz JT, Gray NE. 1948b. A taxonomic revision of *Podocarpus*. II. The American species of *Podocarpus*: section *Stachycarpus*. *Journal of the Arnold Arboretum of Harvard University* **29:** 64–76.

Conran JG, Wood GG, Martin PG, Dowd JM, Quinn CJ, Gadek PA, Price RA. 2000. Generic relationships within and between the Gymnosperm families *Podocarpaceae* and *Phyllocladaceae* based on an analysis of the chloroplast gene *rbc*L. *Australian Journal of Botany* **48:** 715–724.

Doweld AB. 2001. *Botryopitys* – novoe rodovoe nazvanie (*Podocarpopsida*). *Botryopitys*, a new generic name (*Podocarpopsida*). *Turczaninowia* **3:** 37–38.

Fahn A. 1990. *Plant anatomy* (4th edn). Oxford: Pergamon Press.

Farjon A. 2001. *World checklist and bibliography of conifers* (2nd edn). Kew: Royal Botanic Gardens.

Florin R. 1951. Evolution of cordaites and conifers. *Acta Horti Bergiani* **15:** 285–388.

Florin R. 1954. The female reproductive organs of conifers and taxads. *Biological Reviews of the Cambridge Philosophical Society* **29:** 367–389.

Gaussen H. 1974. Les Gymnospermes actuelles et fossiles. Fascicule XIII. Les Podocarpines sauf les *Podocarpus*. *Travaux du Laboratoire Forestière du Toulouse* **2**(1) Partie **2**(3)**:** fasc. **XIII**.

Gibbs LS. 1912. On the development of the female strobilus in *Podocarpus*. *Annals of Botany (Oxford)* **26** (102)**:** 515–571.

Glidewell SM, Möller M, Duncan G, Mill RR, Masson D, Williamson B. 2002. NMR imaging as a tool for noninvasive taxonomy: comparison of female cones of two Podocarpaceae. *New Phytologist* **154:** 197–207.

Glidewell SM, Williamson B, Goodman BA, Chudek JA, Hunter G. 1997. An NMR microscopic study of grape (*Vitis vinifera* L.). *Protoplasma* **198:** 27–35.

Gray NE. 1953. A taxonomic revision of *Podocarpus* VII. The African species of *Podocarpus* section *Afrocarpus*. *Journal of the Arnold Arboretum of Harvard University* **34:** 67–76.

Gray NE, Buchholz JT. 1951a. A taxonomic revision of *Podocarpus* V. The South Pacific species of *Podocarpus*: section *Stachycarpus*. *Journal of the Arnold Arboretum of Harvard University* **32:** 82–92.

Gray NE, Buchholz JT. 1951b. A taxonomic revision of *Podocarpus* VI. The South Pacific species of *Podocarpus*: section *Sundacarpus*. *Journal of the Arnold Arboretum of Harvard University* **32:** 93–97.

Grove GG, Rothwell GW. 1980. *Mitrospermum vinculum* sp. nov., a cardiocarpalean ovule from the Upper Pennsylvanian of Ohio. *American Journal of Botany* **67:** 1051–1058.

Hill RS, Pole MS. 1992. Leaf and shoot morphology of extant *Afrocarpus*, *Nageia* and *Retrophyllum* (Podocarpaceae) species, and species with similar leaf arrangement, from Tertiary sediments in Australasia. *Australian Systematic Botany* **5:** 337–358.

Hilton J, Wang S-J, Tian B. 2003. Reinvestigation of *Cardiocarpus minor* (Wang) Li *nomen nudum* from the Lower Permian of China and its implications for seed plant taxonomy, systematics and phylogeny. *Botanical Journal of the Linnean Society* **141:** 151–175.

Ishida N, Koizumi M, Kano H. 2000. The NMR microscope: a unique and promising tool for plant science. *Annals of Botany* **86:** 259–278.

Jain KK. '1977' publ. 1978. Morphology of female strobilus in *Podocarpus neriifolius*. *Phytomorphology* **27:** 215–233.

Kelch DG. 1998. Phylogeny of *Podocarpaceae*: comparison of evidence from morphology and 18S rDNA. *American Journal of Botany* **85:** 986–996.

Kelch DG. 2002. Phylogenetic assessment of the monotypic genera *Sundacarpus* and *Manoao* (Coniferales: *Podocarpaceae*) utilising evidence from 18S rDNA sequences. *Australian Systematic Botany* **15:** 29–35.

Konar RN, Oberoi YP. 1969. Anatomical studies on *Podocarpus gracilior*. *Phytomorphology* **19:** 122–133.

de Laubenfels DJ. 1978. The genus *Prumnopitys* (Podocarpaceae) in Malesia. *Blumea* **24:** 189–190.

Long A. 1966. Some Lower Carboniferous fructifications from Berwickshire, together with a theoretical account of the evolution of ovules, cupules, and carpels. *Transactions of the Royal Society of Edinburgh* **66:** 345–375.

Masson D, Glidewell SM, Möller M, Mill RR, Williamson B. 2001. Non-destructive utilisation of herbarium material for taxonomic studies using NMR imaging. *Edinburgh Journal of Botany* **58:** 1–14.

Mauseth JD. 1988. *Plant anatomy*. Menlo Park, CA: The Benjamin/Cummings Publishing Co.

Melikian AP, Bobrov AVFCh. 1997. O stroenii narzhnykh pokpovov semyan – epimatiya i arillusa – u predstavitelej semejstva Podocarpaceae. *Byuleten Moskovskogo Obshchestva Ispytatelei Prirody* **102**(5), **C 43:** 43–53. [In Russian.]

Melikian AP, Bobrov AVFCh. 2000. Morfologiya shchenskikh reproduktivi'kh obganov i op't rostroenniya filogeneticheskoj sistemy poryadkov Podocarpales, Cephalotaxales i Taxales. [Morphology of female reproductive structures and

an attempt of the construction of phylogenetic system of orders Podocarpales, Cephalotaxales, and Taxales.] *Botanicheskij Zhurnal (Moscow and Leningrad)* **85** (7)**:** 50–67. [In Russian.]

Mill RR, Möller M, Christie F, Glidewell SM, Masson D, Williamson B. 2001. Morphology, anatomy and ontogeny of female cones in *Acmopyle pancheri* (Brongn. & Gris) Pilg. (*Podocarpaceae*). *Annals of Botany* **n.s. 88:** 55–67.

Möller M, Mill RR, Glidewell SM, Masson D, Williamson B. 2000. Comparative biology of the pollination mechanisms in *Acmopyle pancheri and Phyllocladus hypophyllus* (Podocarpaceae s.1.) and their taxonomic significance. *Annals of Botany* **n.s. 86:** 149–158.

Morvan J. 1980. Analyse comparée de la vascularisation dans les cônes femelles indemnes et parasités (larve de *Cecidomyiidae*, Diptères) chez *Stachycarpus spicata*. *Phytomorphology* **30:** 84–97.

Morvan J. 1983. Étude comparée de la vascularisation dans les ramifications de l'appareil végétatif et du cône femelle chez *Stachycarpus spicata* R. Brown, Podocarpacées. *Flora* **173:** 49–62.

Morvan J. 1990. Ontogenèse et phylogénie comparées du cône femelle chez *Saxegothaea conspicua* Lindl. Saxegothaeacées et *Microcachrys tetragona* Hook. Podocarpacées. *Comptes Rendus de l'Académie des Sciences du Paris, Sér. 3, Sciences Vie* **310:** 651–656.

Napp-Zinn K. 1966. Anatomie des Blattes. I. Gymnospermen. *Handbuch der Pflanzenanatomie* **8:** 1–369.

Orr MY. 1944. The leaf anatomy of *Podocarpus*. *Transactions and Proceedings of the Botanical Society of Edinburgh* **34:** 1–54.

Page CN. 1989. New and maintained genera in the conifer families Podocarpaceae and Pinaceae. *Notes from the Royal Botanic Garden Edinburgh* **45:** 377–395.

Page CN. 1990. Podocarpaceae. In: Kubitzki K, ed. *The families and genera of vascular plants, 1, pteridophytes and gymnosperms.* (Kramer KU, Green PS, eds). Heidelberg: Springer, 332–346.

Sahni B, Mitra AK. 1927. Notes on the anatomy of some New Zealand species of *Dacrydium*. *Annals of Botany* **41:** 75–89.

Sinclair WT, Mill RR, Gardner MF, Woltz P, Jaffré T, Preston J, Hollingsworth ML, Ponge A, Möller M. 2002. Evolutionary relationships of the New Caledonian heterotrophic conifer, *Parasitaxus usta* (*Podocarpaceae*), inferred from chloroplast *trn*L-F intron/spacer and nuclear rDNA ITS2 sequences. *Plant Systematics and Evolution* **233:** 79–104.

Sinnott EW. 1913. The morphology of the reproductive structures in the *Podocarpineae*. *Annals of Botany (König and Sims)* **27:** 39–82.

Sporne KR. 1965, 1974. *The morphology of gymnosperms*. Ed. 1, 1965; Ed. 2, 1974. London: Hutchinson Ltd.

Stevenson DW. 1990. Morphology and systematics of the *Cycadales*. *Memoirs of the New York Botanical Garden* **57:** 8–55.

Tarbaeva VM. 1997. Stroenie semyan rastenij semeistva Podocarpaceae. [Structure of seeds and seed coat of species from Podocarpaceae family.] *Byulleten' Glavnogo Botanicheskogo Sada* **174:** 104–115.

Thomasson JR. 1997. Grass starch grains. http://www.fhsu.edu/biology/thomasson/starch.htm.

Tomlinson PB. 1992. Aspects of cone morphology and development in Podocarpaceae (Coniferales). *International Journal of Plant Sciences* **153:** 572–588.

Tomlinson PB. 1994. Functional morphology of saccate pollen in conifers with special reference to Podocarpaceae. *International Journal of Plant Sciences* **155:** 699–715.

Tomlinson PB, Takaso T. 2003. Seed cone structure in conifers in relation to development and pollination: a biological approach. *Canadian Journal of Botany* **80:** 1250–1273.

Turner GW. 1999. A brief history of the lysigenous gland hypothesis. *Botanical Review* **65:** 76–88.

Wen TH, He XL. 1989. The morphology of fruits and starches in bamboo and their systematic value. *Acta Phytotaxonomica Sinica* **27:** 365–377. [In Chinese; English summary.]

Wen TH, He XL. 1991. Fruit morphology and starches in bamboo fruits and their systematic position. In: Rao AN, Zhang XP, Zhu SL, eds. *Selected papers on recent bamboo research in China*. Beijing: Bamboo Information Centre, Chinese Academy of Forestry, 47–59.

Zhong R, Taylor JJ, Ye Z-H. 1999. Transformation of the collateral vascular bundles into amphivasal vascular bundles in an *Arabidopsis* mutant. *Plant Physiology* **120:** 53–64.